Bachelor Thesis

Bose-Einstein condensates in magnetic microtraps with attractive atom-atom interactions

Florian Atteneder
1331379

Supervisor: Ao.Univ.-Prof. Mag. Dr. Ulrich Hohenester

University of Graz
Institute of Physics

January, 2017

Abstract

Controlling Bose-Einstein condensates (BECs) that are confined by magnetic microtraps is a major challenge in modern physics. Such BECs allow us to study quantum mechanical effects on a macroscopic scale.

One of the most essential properties of BECs is the atom-atom interaction, which characterizes the behavior of atoms within such a condensate. It influences how BECs respond to external manipulations. The first part of this thesis deals with a discussion about the basic principles of BECs as well as its mathematical description. Also a short side note about atom chips is provided, which is a device that is used in recent experiments for efficient trapping of BECs. The investigations rely on optimization results that were obtained with the MATLAB toolbox OCTBEC. With this tool it is possible to simulate BECs under manipulations. The actual investigation deals with simulation results that were obtained for a splitting process of a BEC where attractive interactions are present. This thesis gives a statement about how well the OCTBEC toolbox is applicable for the derivation of control strategies to split BECs with attractive interactions.

Contents

Chapter 1

Introduction

Control of quantum systems is required to develop more complex quantum technologies, e.g. quantum computers or quantum cryptography devices. Bose-Einstein condensates (BECs) allow investigations of quantum effects on a macroscopic scale. To investigate such effects one has to be able to control BECs efficiently in experiments.

The Atomchip Group[1] from the Technical University of Vienna examined the behavior of Bose-Einstein condensates trapped above the surface of a so-called atom chip. Atom chips allow efficient trapping of ultra cold atoms with small currents running through chip wires. One goal of this research project is to manipulate BECs in a way that they are transferred from an initial state to a desired state within a distinct time. This is achieved by a manipulation with an external magnetic field. To achieve an efficient transfer, a suitable control strategy for the control field is required. Such strategies can be obtained by numerical simulations.

The theoretical modeling of BEC manipulations was done at the University of Graz and the Technical University of Vienna. A MATLAB toolbox was developed which performs simulations of BECs trapped and controlled in magnetic microtraps. The operation scheme of this toolbox is based on two powerful devices: One is optimal control theory (OCT), which is a mathematical tool for solving inverse problems. The second tool is the Gross-Pitaevskii-Equation, which is a nonlinear generalized Schrödinger equation (GSE) for macroscopic wave functions. This equation describes the physics behind the behavior of BECs. The combination of these devices was implemented in the `MATLAB` toolbox OCTBEC [1].

One specific application of OCTBEC is to derive control strategies to split a BEC from a single cluster into two separated parts. This is achieved by varying an external confinement potential with time. The confined BECs are characterized by a parameter that describes how strong the atoms interact with one another in a condensate. This interaction influences the BECs in a way that they responds differently to external manipulations. In the case of repulsive interactions, the derivation of control strategies works out well. But an investigation of the OCTBEC toolbox for the derivation of strategies for the case of attractive interactions is not available. The goal of this thesis

[1]Webpage: http://atomchip.org/

is to give a statement about whether the toolbox is applicable to derive efficient control strategies in this case or not. Therefore, exemplary control strategies were computed and then analyzed.

The following text is organized as follows: Chapter 2 covers the basic properties of BECs, a side note about atom chips and the mathematical description of BECs. In chapter 3 the operation principle of OCT and the structure of the OCTBEC toolbox is discussed. After this, we present the investigation method that is used for analyzing the obtained strategies in chapter 4. The actual investigation of these strategies is then given in chapter 5 and a conclusion is drawn in chapter 6.

Chapter 2

Theory

The first part of this thesis contains a discussion about the basic properties of bosons and BECs. This chapter also contains a side note about atom chips. The covered topics are limited to the required knowledge for the following chapters, where we deal with the behavior, operation methods and solutions of optimal control theory (OCT) combined with the Gross-Pitaevskii equation (GPE).

This chapter is structured as follows: Section 2.1 deals with bosons and fermions and their characteristics. This information is required to describe the principle how to realize condensation of bosonic atom clouds, which is described in section 2.2. After this, in section 2.3 we introduce to atom chips, and section 2.4 lists the mathematical description of BECs.

2.1 Bosons and fermions

Before we can answer the question how a BEC is realized, we have to learn more about quantum particles and their characteristics. Quantum particles differ from classical particles in the way that they cannot be distinguished if they are of the same species. Quantum statistic is a theory that describes ensembles consisting of indistinguishable particles. Within quantum statistic, quantum particles are divided in two classes of particles, namely bosons and fermions. Each of these classes is of fundamental importance. In the following, the definition of bosons and fermions as well as their corresponding statistics are given.

As already mentioned, a the physical properties of a system must not change if two indistinguishable particles are interchanged. This means that the following condition for the total probability distribution of a system consisting of two identical quantum particles must hold:

$$|\psi(\vec{r}_1, \vec{r}_2)|^2 = |\psi(\vec{r}_2, \vec{r}_1)|^2, \tag{2.1}$$

$\psi(\vec{r}_1, \vec{r}_2)$ is the system wave function that depends on the position vectors $\vec{r}_1$ for particle 1 and $\vec{r}_2$ for particle 2. This condition states that the probability density of a set of indistinguishable particles remains invariant when interchanging any two particles.

There are only two possible wave functions that can fulfill this equation. The first possible wave function is

$$\psi(\vec{r}_1, \vec{r}_2) = \psi(\vec{r}_2, \vec{r}_1). \tag{2.2}$$

This is a so-called symmetric wave function, because its global phase factor is $e^{i2\pi n} = 1$, n is an integer. The other possibility that fulfills (2.1) is

$$\psi(\vec{r}_1, \vec{r}_2) = -\psi(\vec{r}_2, \vec{r}_1) \tag{2.3}$$

which is called a antisymmetric wave function. Its global phase factor is $e^{i2\pi n} = -1$, n is a half-integer.

In the past century two important statistics that describe the mean occupation number of indistinguishable particles were introduced. The first one is the so-called Bose-Einstein statistic, which takes a set of indistinguishable particles into account that belong to equation (2.2). The statistic is:

$$\bar{n}_\nu = \frac{1}{e^{\beta(\epsilon_\nu - \mu)} - 1}, \tag{2.4}$$

$\bar{n}_\nu$ is the mean occupation number of particles in a quantum state ν with energy ϵ_ν at thermal equilibrium. μ is the chemical potential, β is a normalization factor that depends on temperature. All particles that are subjected to the Bose-Einstein statistic are called bosons.

The statistic that describes the mean occupation number of indistinguishable particles that belong to equation (2.3) is called Fermi-Dirac statistic and it is defined by:

$$\bar{n}_\nu = \frac{1}{e^{\beta(\epsilon_\nu - \mu)} + 1}. \tag{2.5}$$

We call particles that belong to the Fermi-Dirac statistic fermions.

From the spin-statistic theorem [2] follows that all bosons have integer spin and all fermions have half-integer spin. There are several other characteristics of bosons and fermions, but a more detailed discussion about them is not required for the following sections.

On the basis of this theorem, a boson can be constructed by combining an even number of fermions in one particle. This construction takes the Pauli exclusion principle into account. This principle states that two identical fermions cannot occupy the same quantum state simultaneously, but bosons can. Helium-4 (^{4}He) is one example that behaves as a boson. It consists of two protons, two neutrons and two electrons. Protons, neutrons and electrons are fermions with spin 1/2 $\hbar$. Each pair of identical particles then combines with +1/2 $\hbar$ and -1/2 $\hbar$ spin to a total spin of zero. Because the total spin is zero, ^{4}He behaves as a boson. Helium-4 is well known due to its application as a superfluid, which is based on the BEC phenomenon. It has to be mentioned that the treatment of a combination of fermions as a boson only applies on a scale of size that is greater than the spacing between the fermions. Otherwise the particles would not obey the Pauli exclusion principle.

2.2 Bose-Einstein condensation

As the name Bose-Einstein condensation suggests, this state of matter was theoretically discovered by Satyendranath Bose and Albert Einstein. The prediction of BECs was published in 1924. The following lines cover a derivation of the BEC that follows the lecture notes from [3].

For explaining the process of Bose-Einstein condensation, we take a set of spinless[1] bosons. The mean number of bosons $\bar{N}$ in a closed system is the sum over the mean number of particles $\bar{n}_\nu$ in quantum states ν with energy ϵ_ν

$$\bar{N} = \sum_\nu \bar{n}(\epsilon_\nu). \tag{2.6}$$

It is possible to replace the sum over discrete quantum states by an integral and introduce the density of states $D(\epsilon)$. Using (2.4) for the mean number of particles that occupy quantum state ν with energy ϵ_ν, $\bar{N}$ is then given by

$$\bar{N} = \int_0^\infty \bar{n}(\epsilon_\nu) D(\epsilon) d\epsilon. \tag{2.7}$$

The density of states (see figure 2.1) in 3 dimensions as a function of energy ϵ is given by:

$$D(\epsilon) = C\epsilon^{1/2}, \tag{2.8}$$

$C = (2m)^{3/2}/(4\pi^2\hbar^3)$ is a constant factor. m is the effective particle mass and $\hbar$ is the reduced Planck constant. From equation (2.7) we obtain the particle density as a function of μ

$$\rho(\mu) = \frac{\bar{N}}{V} = C \int_0^\infty \frac{\epsilon^{1/2}}{e^{\beta(\epsilon-\mu)} - 1} d\epsilon, \tag{2.9}$$

V is the volume that contains all particles. Before continuing with the evaluation of the integral, it has to be checked which values μ can take: Assume the ground state energy ϵ_0 ($\nu = 0$) to be zero, then the mean occupation number of the ground state is

$$\bar{n}_0 = \frac{1}{e^{-\beta\mu} - 1}. \tag{2.10}$$

If $\mu > 0$ the mean occupation number of the ground state would be negative, which is unphysical. For $\mu = 0$, the expression is not determined. It follows

$$\mu \overset{!}{<} 0. \tag{2.11}$$

The next step is to increase the particle density for constant temperature. To do so, we have to increase the chemical potential μ, because (2.9) is strictly increasing within

[1] Spinless bosons are particles where the intrinsic angular momentum is zero, e.g. ^{4}He. This is because for spinless bosons there is only one species (total spin zero) in contrast to bosons with spin (two species: spin up and spin down).

the interval $\mu \in (-\infty, 0)$. From the condition (2.11) follows that the maximum value of μ is zero and (2.9) can be rewritten as

$$\rho_C = C\beta^{-3/2} \int_0^\infty \frac{x^{1/2}}{e^x - 1} dx = \frac{(2mk_BT)^{3/2}}{4\pi^2\hbar^3} \times 2.612. \tag{2.12}$$

We used the dimensionless substitution $x = \beta\epsilon$. $\beta = 1/(k_BT)$ is constant factor, k_B is the Boltzmann constant and T is the temperature. This result is a finite number and we refer to it as the maximum particle density. But what happens when the particle density ρ is already lager than the maximum particle density ρ_C? Where have the 'surplus bosons' gone? The answer is that they have gone into the ground state. The source of this paradox lies in the replacement of the sum from equation (2.6) by an integral, which has to be treated more carefully. The resolution to this is a separation of the particle density into the one for the ground state ρ_0 and one for all excited states ρ_{ex}:

$$\rho = \rho_0 + \rho_{ex} = \frac{\bar{n}_0}{V} + \frac{\bar{n}_{ex}}{V}, \tag{2.13}$$

$\bar{n}_0, \bar{n}_{ex}$ are the mean numbers of particles that occupy the ground state and all excited states respectively.

Again, we set $\epsilon_0 = 0$ and use the integral expression from (2.9) for ρ_{ex}:

$$\rho = \frac{1}{V}\frac{1}{e^{-\beta\mu} - 1} + C\int_0^\infty \frac{\epsilon^{1/2}}{e^{\beta(\epsilon-\mu)} - 1} d\epsilon. \tag{2.14}$$

Assuming μ to be very close to zero, but still a negative number, then the first term in (2.14) can be approximated by

$$e^{-\beta\mu} - 1 \simeq 1 - \beta\mu. \tag{2.15}$$

With this and the result from (2.12) the total particle density then is

$$\rho = -\frac{k_BT}{\mu V} + \frac{(2mk_BT)^{3/2}}{4\pi^2\hbar^3} \times 2.612. \tag{2.16}$$

From this expression it is easy to see what happens when the particle density is raised above ρ_C - the first term gets arbitrarily large when μ goes toward zero (μ is still a negative number) and ρ will be dominated by the particle density of the ground state ρ_0. It is exactly the increase of the total particle density that forces bosons to occupy the ground state. The entity of particles that now occupy the ground state are called Bose-Einstein condensate.

This derivation is valid for bosons in 3 dimensions. One may now ask if Bose-Einstein condensation is possible in lower dimensions. Let's consider the case for 2 dimensions. The density of states (see figure 2.1) is a constant $D(\epsilon) \propto \epsilon^0$ and the total particle density ρ as a function of μ then is

$$\rho(\mu) \propto \int_0^\infty \frac{1}{e^{\beta(\epsilon-\mu)} - 1} d\epsilon \to \infty. \tag{2.17}$$

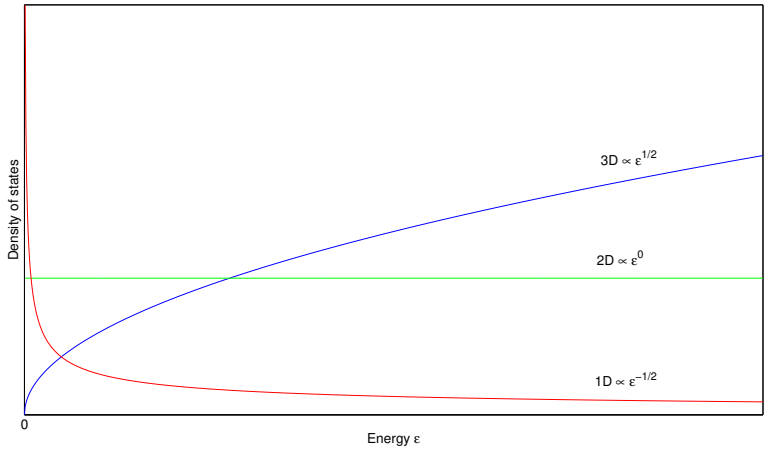

Figure 2.1: Density of states $D(\epsilon)$ in different dimensions: Only the density of states in 3 dimensions (blue line) vanishes, when the energy goes towards zero; In 2 dimensions the density of states is a constant for every energy value (green line); In 1 dimension the density of states goes towards infinity when the energy approaches zeros (red line);

This means that the maximum total particle density is unlimited. It follows that it is impossible to fill all states and force surplus particles to occupy a specific state with a macroscopic number of particles, as in the case of 3 dimensions.

The same argument also holds for the case of 1 dimension, where the density of states (see figure 2.1) is $D(\epsilon) \propto \epsilon^{-1/2}$. The corresponding total particle density ρ then is

$$\rho(\mu) \propto \int_0^\infty \frac{\epsilon^{-1/2}}{e^{\beta(\epsilon-\mu)} - 1} d\epsilon \to \infty. \tag{2.18}$$

Again, it is not possible to completely fill all states so that the 'surplus bosons' are forced to occupy the ground state. This means that in both cases no BEC can be formed by increasing the particle density.

The failure of Bose-Einstein condensation in 1 and 2 dimensions holds for a set of bosons in free space, but it is possible to produce a so-called quasi-condensate in 1 and 2 dimensions. This can be achieved by applying a suitable confinement potential to the bosons that modifies the density of states in a way that the maximum particle density approaches a finite number.

Before we end this section we introduce the temperature where Bose-Einstein condensation occurs. To start this, we define the thermal de Broglie wavelength

$$\lambda_T = \left(\frac{2\pi\hbar^2}{m k_B T} \right)^{1/2}. \tag{2.19}$$

This wavelength is the mean de Broglie wavelength of particles in an ideal gas, for a specific temperature T. If λ_T is on the order of or lager than the interatomic spacing between the particles quantum effects start to play an essential role. In the other

case, where λ_T is smaller than the mean distance between the particles, the system is dominated by classical effects.

By inserting (2.19) into equation (2.12) the condensation temperature can be calculated by

$$T_C = \frac{2}{\pi^{1/2}} \frac{1}{{\lambda_T}^3} \times 2.612. \tag{2.20}$$

T_C marks the transition between the presence of quantum and classical effects, depending on λ_T. At $T = T_C$ the thermal de Broglie wavelength equals the average particle spacing which is about $(V/N)^{1/3}$. V is the volume and N is the number of particles.

Further information about the process of Bose-Einstein condensation as well as the characteristics of BECs can be read in [4, 5].

2.3 Atomchips

A Bose-Einstein condensate was first produced in 1995 by E. Cornell and C. Wieman at the University of Colorado [6] and by W. Ketterle at the Massachusetts Institute of Technology. They received the Nobel Prize in Physics in 2001. The Bose-Einstein condensate was predicted in 1924. Why did it take more than 70 years from theoretical discovery of the BEC to experimental verification?

The physicists from the last century had to overcome some major challenges to realize BECs in experiments. This section summarizes shortly the techniques that enabled the cooling of matter to temperatures close to absolute zero. It also contains an introduction to atom chips and their purpose for what they were developed.

Typical values for the condensation temperature T_C of a BEC are in the range of hundreds of nK absolute temperature. To cool down matter to such low temperatures was one difficulty to overcome for the physicists before the experimental realization of BECs. The key to this was the development of the laser cooling technique and the evaporative cooling technique. Each of this techniques rely on a simple mechanism.

Temperature is related to disordered motion of particles. Laser cooling takes use of the momentum of photons to reduce disordered motion of particles. This is done by shining photons onto an atom cloud. When these photons are scattered by the atom cloud's particles each atom suffers a recoil due to absorption and emission processes caused by the photons. Due to the Doppler effect, only photons that move towards the atoms direction of motion cause a recoil on the atoms itself. This recoil is then directed in the opposite direction of the atoms momentum, which reduces its momentum. This causes a decrease of the disorder motion of all particles. As a consequence, the temperature of the system is lowered.

The evaporative cooling technique makes it possible to fill the gap between the lower limit of cooling achieved by laser cooling and the required critical temperature. This is done by a process that sorts out particles with high momentum. Imagine a cloud of atoms confined by an external controllable confinement potential. The potential walls

are characterized by a finite height, which means that particles can escape the potential if their momentum is high enough. Now we are going to lower the potential walls in defined steps. With each step particles with an energy that is higher than the potential walls will jump out from the confinement potential. Again, the reduction of the momentum reduces the disordered motion. It follows that the temperature of the confined ensemble is lowered.

Beside the issues of cooling matter to low temperatures, also perturbations like undesirable radiation or interactions between particles in the atom cloud have to be controlled for the realization of BECs. One approach to circumvent these issues was the development of the concept of atom chips. Before this approach was made, research groups used experimental setups for BECs that required huge facilities to store all needed devices. Atom chips enabled them to reduce the complexity of such setups. The cooling of atom clouds became even easier, because the vacuum chambers that contain the BECs could be made smaller. The development of atom chips can somehow be seen as another major approach that enabled us access to the research field of BECs.

But how is it possible to trap and confine atom clouds onto an atom chip? An atom chip is nothing else then a chip that contains wires which carry currents and produce magnetic fields. The Biot-Savart law enables the description of the magnetic field produced by moving electric charges. In the case of an infinite long wire that carries a current $\vec{I}$, the magnetic field $\vec{B}$ [2] at a point P separated by $\vec{r}$ is given by

$$\vec{B}(\vec{r}) = \frac{\mu_0 \vec{I}}{2\pi|\vec{r}|}\vec{e}_\varphi. \tag{2.21}$$

μ_0 is the magnetic permeability of free space and $\vec{e}_\varphi$ is the radial unit vector that is perpendicular to the wire axes. This equation states that the magnetic field strength is inverse proportional to the distance $|\vec{r}|$. It is exactly this characteristic of the Biot-Savart law that led to the development of atom chips. Because of this inverse relation, small currents cause high magnetic fields only a few μm above the surface of an atom chip. The strong magnetic field then allows easy trapping of BECs above the atom chips surface.

To end this section a short side note about the design of atom chips is given. Atom chips that are used nowadays are micro-fabricated chips. A picture of an atom chip module is shown in figure 2.2(a). The dark mirrored surface on the top of this module is the atom chip itself. If one takes a closer look at the atom chip, some features of the wire layout that is given in figure 2.2(b) can be seen. At the center of the chip the wires cross, which requires that the wires are arranged on different layers. This means that some wires are assembled within a layer that is insulated by polyimide pads from a second layer containing different wires. Such a design allows the arrangement of a whole bunch of wires within a chip.

[2] Following common use, the magnetic induction $\vec{B}$ names the "magnetic field".

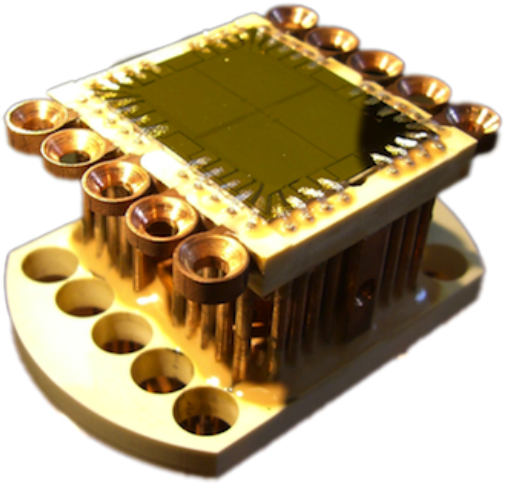

(a) This module will be mounted on an apparatus, and will be then installed in a vacuum chamber. Some features of the schematic wire layout (right figure) can be seen on the top of this module. (source: *www.atomchip.org*)

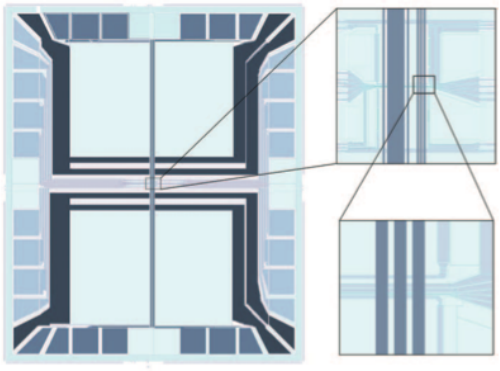

(b) The dark blue contours mark wires that provide the longitudinal confinement. The blue wires running from the top to the bottom are responsible for the trapping of atoms. The wires are arranged on different layers and separated by polyimide pads. (source: [7])

Figure 2.2: Atom chips were one major approach that gained us access to the research field of BECs. (a) Picture of an atom chip module. (b) Schematic wire layout of an atom chip.

In general, the geometry of a wire is responsible for the corresponding field geometry it can create. For example, Z-shaped wires produce a harmonic oscillator potential with a nonzero field at the minimum. In contrast, U-shaped wires create a spherical quadrupole field. Due to this, multilayer chips often contain a wide diversity of different wire geometries. With this feature only one atom chip is needed to perform different experiments that require different field geometries. A more detailed discussion about traps and wire geometries of micro-fabricated chips is given in [8].

To estimate the size of an atom chip, we provide dimensions of some features of such a chip. The atom chip from figure 2.2 has a size of 25 $\times$ 30 mm. The dark blue confinement wires have a width of 500 μm. The three parallel wires that a presented in the lower right inset in figure 2.2(b) have a width of only 10 μm and are separated by a 300 nm wide gaps. To produce a structure with such small features, accurate manufacturing techniques are required. Due to the availability of mature technologies like optical ultraviolet lithography and e-beam lithography, it is possible to fabricate chips with such small features.

There are two last things that should be added to this section that are related to figure 2.2(a). First, one can see that there are 10 rings on top of the module and also 10 holes in the base plate of the module. This features belong to a clever cooling system

of the chip since very small temperatures are required for the condensation of bosons. Therefore, every heat source within the experimental setup and near the BEC is undesired. The currents that run through the wires of the chip can scale up to 100 A, which means that heat will be produced and then be radiated by the chip surface. Since the condensate is trapped only a few μm above the chip surface, the produced heat has to be dissipated, otherwise the atom cloud cannot condensate. The second important thing about an atom chip is its mirrored surface. Laser cooling requires to shine photons from all directions on the atom cloud. Because the chip itself prevents to shine photons from the chip side onto the condensate, the mirrored surface also allows to irradiate the condensate from this side.

More details about atom chips as well as the experiments from the Atomchip Group are available in [9, 7] and on *www.atomchip.org*.

2.4 Gross-Pitaevskii equation

In section 2.2 properties of Bose gases where discussed under the assumption that there are no atom-atom interactions between the particles. These properties can be transferred with marginal change to non-uniform Bose gases used in recent experiments, like in the experiment of the Atomchip Group. But when one would like to compute the wave function of the ground state of a BEC, interatomic interactions come up to play an essential role.

The time-independent (stationary) Gross-Pitaevskii equation (GPE) is a mean field approach[3] for the description of BECs with atomic interactions. It is given by the following equation:

$$\mu\psi(\vec{r}) = \left(-\frac{\hbar^2}{2m}\nabla^2 + V_{ext}(\vec{r}) + \kappa|\psi(\vec{r})|^2\right)\psi(\vec{r}), \tag{2.22}$$

μ is the chemical potential, $\psi(\vec{r})$ the wave function, m the particle mass, $V_{ext}(\vec{r})$ the external trapping potential. Equation (2.22) is a generalized time-independent (stationary) Schrödinger equation which includes a nonlinear term $\kappa|\psi(\vec{r})|^2$. Note that the eigenvalue of the time-independent GPE is the chemical potential μ, not the energy per particle as for the time-independent general Schrödinger equation (GSE). When $\kappa = 0$, the stationary GPE becomes the stationary GSE and the chemical potential μ is then equal to the eigenvalue of the time-independent GSE.

κ characterizes the atom-atom interactions. It is defined as

$$\kappa = \frac{4\pi\hbar^2 a}{m}, \tag{2.23}$$

[3] Mean field theory is an approach for many-body systems where the influences and interactions between all components is averaged and replaced by a single parameter [4].

a is the s-wave scattering length of the Bose gas, which only depends on two-body interactions between the particles for low temperatures. Generally, values of $\kappa > 0$ characterize repulsive interactions between the atoms, whereas values of $\kappa < 0$ indicate that the atoms are influenced by attractive interactions between one another. Since κ and a are directly linked by equation (2.23), values of $a > 0$ represent repulsive interactions and $a < 0$ represents attractive interactions. It has to be mentioned that this term highly effects the condensation and the stability of BECs. It was shown that κ cannot take every possible value, because the atom-atom interaction can cause loss of trapped atoms due to state transitions. Due to the complexity of this topic a detailed discussion is left out. We refer the interested reader to [10, 11, 12, 13].

The solution for the ground state of the time-independent GPE for $\kappa = 0$ and a harmonic oscillator potential of the form

$$V_{ext}(\vec{r}) = \frac{m}{2}(\omega_x^2 x^2 + \omega_y^2 y^2 + \omega_z^2 z^2), \tag{2.24}$$

with ω_i as the oscillator frequencies for the i-th dimension, is a Gauss package

$$\psi(\vec{r}) = \left(\frac{m\omega_{ho}}{\pi\hbar}\right)^{\frac{3}{4}} exp\left[-\frac{m}{2\hbar}(\omega_x x^2 + \omega_y y^2 + \omega_z z^2)\right]. \tag{2.25}$$

ω_{ho} is the average of the oscillator frequencies

$$\omega_{ho} = (\omega_x \omega_y \omega_z)^{\frac{1}{3}}. \tag{2.26}$$

The average width of this Gauss package is the harmonic oscillator length

$$a_{ho} = \sqrt{\frac{\hbar}{m\omega_{ho}}}. \tag{2.27}$$

The solution (2.25) of the time-independent GSE is well known as the ground state of a particle in a three dimensional harmonic well potential and is independent of the s-wave scattering length a.

If $\kappa \neq 0$, the GPE becomes a nonlinear ordinary differential equation and therefore hard to solve with analytical methods. Numerical calculations are often used to obtain solutions in this case. These solutions are then also Gauss packages, but with different widths. This is due to the fact that the interatomic interaction is part of the GPE and, as equation (2.23) states, related with s-wave scattering length. Figure 2.3 shows numerical solutions of the time-independent GPE for different values of $N|a|/a_{ho}$. This fraction compares the interaction energy with the kinetic energy of the particles. E.g. in figure 2.3(a) the wave function with $N|a|/a_{ho} = 0.5$ indicates a higher particle density compared to the solution in figure 2.3(b) for $N|a|/a_{ho} = 100$. This is what one would expect, because values of $\kappa < 0$ force the particles in the BEC to contract, where values $\kappa > 0$ push them apart.

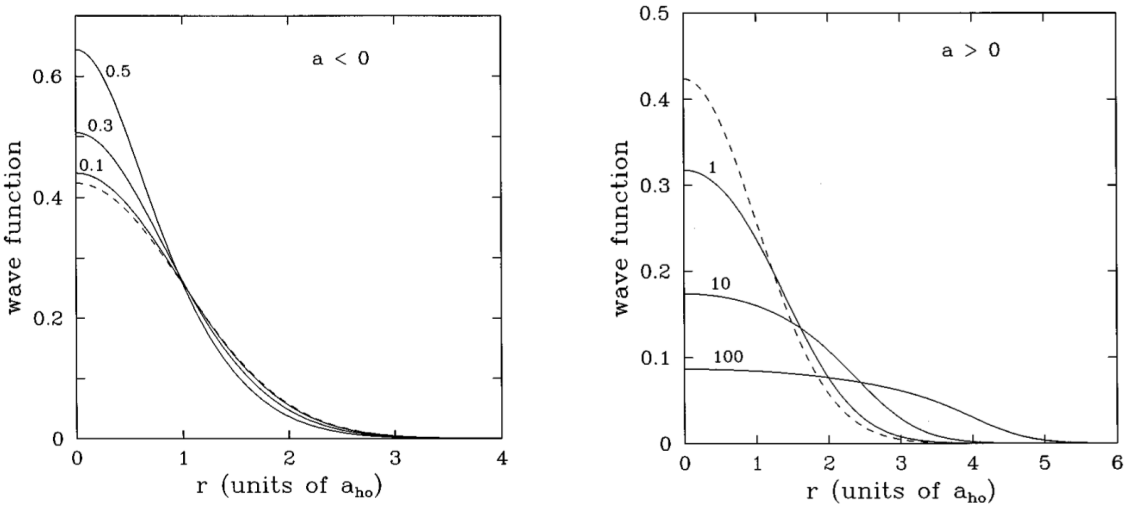

(a) $a < 0 \sim \kappa < 0$ (b) $a > 0 \sim \kappa > 0$

Figure 2.3: BEC wave functions determined by numerical solution methods of the time-independent GPE (2.22) for different values of $N|a|/a_{ho}$: (a) Attractive interactions ($N|a|/a_{ho} = 0.1,0.3,0.5$); (b) Repulsive interactions ($N|a|/a_{ho} = 1,10,100$); Dashed lines show wave function of the time-independent GSE ($a = 0 \sim \kappa = 0$); (source: [4])

The time-dependent Gross-Pitaevskii equation plays a major role for computing the time evolution of the ground state when a BEC is manipulated by varying the confinement potential $V_{ext}(\vec{r}, t)$ over time. The time-dependent GPE is given by:

$$i\hbar\frac{\partial\psi(\vec{r},t)}{\partial t} = \left(-\frac{\hbar^2}{2m}\nabla^2 + V_{ext}(\vec{r},t) + \kappa|\psi(\vec{r},t)|^2\right)\psi(\vec{r},t). \tag{2.28}$$

It is derived from (2.22) by replacing the chemical potential μ with $i\hbar\frac{\partial}{\partial t}$. Note, that in the case of $\kappa = 0$, equation (2.28) transforms to the time-dependent Schrödinger equation which describes the time evolution of non interacting atoms. Once again, values of κ greater (less) than zero indicate repulsive (attractive) interactions between the atoms. If such interactions are present, equation (2.28) is characterized as a nonlinear partial differential equation which is hard to solve with analytical methods. Most of the time numerical calculation methods are used to obtain solutions for the time evolution of BECs.

This was a short overview about the mathematical description of BECs. More information about the GPE as well as atom-atom interactions within BECs is available in [4, 5].

A final remark about the interaction term κ and the s-wave scattering length a has to be given here: We are going to present simulation results that were obtained for different values of κ respectively a. The tuning of this parameters can be done by using so-called

Feshbach resonances. This effect relies on two-body physics and scattering theory and therefore requires advanced knowledge. A discussion of Feshbach resonances is left out, because this would go beyond the scope of this thesis. But we refer the interested reader to [10].

Chapter 3

MATLAB toolbox - OCTBEC

The `MATLAB` toolbox OCTBEC is a numerical tool for simulating the dynamics of BECs under manipulation. It is based on optimal control theory (OCT) and on the Gross-Pitaevskii equation (GPE). The combination of these two components leads to a powerful numerical tool, which is called optimal quantum control of Bose-Einstein condensates (OCTBEC).

In this chapter we discuss the following topics: Section 3.1 deals with the basic idea of OCT. An application of this method will be presented in more detail in section 3.2. At the end, in section 3.3 we present results obtained from the toolbox. These results gave reason for a detailed investigation of the OCTBEC toolbox, which led to this thesis.

3.1 Optimal control theory

To start this section we give an example of a so-called inverse problem. This example should illustrate the need of OCT. Let us think about the following: A company has to produce a certain amount of goods every month. To produce them many different manufacturing processes can be used independently of one another. The difference between these processes is the amount of output on goods and the production costs per good. The business objective for the company is to minimize the production costs and therefore maximize the income. It is clear that there are many possible ways to combine the manufacturing processes to reach the required output on goods per month. But as the business objective states, the costs have to be minimized.

This task is an inverse problem. It is mainly characterized by two parameters: The first one is the initial state. In this example the initial state can be seen as the set of available manufacturing processes together with the required resources that are needed for the goods. The desired state is characterized as the outcoming goods. The goal is to find a production strategy that tells which manufacturing processes should be used for each manufacturing step to produce the desired goods. In addition, the strategy has to be improved, so that the costs per good approach a minimum. This is where OCT starts to play a role. It enables the calculation of an efficient production strategy.

A more general description of an inverse problem would be: To solve an inverse problem one has to find a way to transfer a given system from its initial state to a final state. The final state should match the desired state as good as possible.

To find an appropriate control strategy, it is common to introduce a so-called cost functional J. This functional rates the mismatch between the final and desired state. In terms of the manufacturing example, you can think of J as the costs you have to account for if not all goods are perfect or if certain manufacturing processes are not used optimally.

The task for deriving an efficient control strategy is to minimize J. But when do we call a strategy efficient? One has to set a limiting value for J to decide whether it is efficient or not. In the above example, the head of the company will decide if the costs of a certain strategy are small enough. It has to be mentioned that no reference value can be given for J, because it depends on many factors. The name optimal control theory refers to the optimal control strategy, which is a control strategy where the corresponding cost functional is minimal. This means that the final state exactly matches the desired state. In some applications an optimal strategy cannot be obtained, but several efficient strategies can be found. If the cost for a strategy is then very close to zero, it is often referred to as an optimal control strategy.

OCT applied to actual problems often leads to a complex system that is described by nonlinear equations. Therefore, numerical calculations are needed to obtain appropriate solutions. Nowadays, a diversity of approaches to solve inverse problems by OCT are available. They mainly differ in the way of minimizing the cost functional J. A detailed discussion about different OCT methods is left out, because of the complexity of this topic. But to make the mentioned aspects of OCT clear we discuss the operation method of OCTBEC in the next section.

3.2 Optimal quantum control of Bose-Einstein condensates

Optimal quantum control of Bose-Einstein condensates is the combination of OCT and the GPE (equations (2.22), (2.28)). They were combined in a MATLAB toolbox called OCTBEC. The purpose of this toolbox is to simulate manipulations of BECs. In more detail, the toolbox calculates control strategies that transfer a BEC from an initial state to a desired state. The task of OCT within OCTBEC is to make this transition respectively the control strategy as efficient as possible. This is a typical inverse problem. In this section we discuss the cost functional J, the set of equations that have to be fulfilled for an optimal control strategy as well as the operation procedure of the OCTBEC toolbox.

As already mentioned, it is common to introduce a cost functional to rate the mismatch

between final and desired states. In OCTBEC this functional was defined as

$$J(\psi(T),\lambda) = \frac{1}{2}||\psi(T)-\psi_d||^2 + \frac{\gamma}{2}\int_0^T \left(\dot{\lambda}(t)\right)^2 dt, \tag{3.1}$$

$\psi(T)$ is the final state at terminal time T (= time when the manipulation is over) and ψ_d is the desired state. λ denotes the control parameter and is a function of time t, $\dot{\lambda}(t)$ is the time derivative of λ and γ is a constant number. The physical representation of the final and desired states $\psi(T), \psi_d$ are wave functions and $\lambda(t)$ represents the shape of the confinement potential at time t (this will be discussed in the next section).

The cost functional $J(\psi(T),\lambda)$ consists of two parts: The first one rates the match between the final and desired state at terminal time T. The second one rates the change of λ over time t. This additional term adds extra costs to strategies where λ shows strong variations or even discontinuities. Therefore, continuous control parameters with small variations will be derived more likely, because of their lower costs. γ is a parameter that rates the importance of the additional term and is usually set to $\gamma \ll 1$.

The main task is now to minimize J. To do this, a Lagrange multiplier $p(x,t)$ together with a Lagrange function $L(\psi,p,\lambda)$ is introduced:

$$L(\psi,p,\lambda) = J(\psi,\lambda) + \Re\mathfrak{e}\left[\int_0^T \left\langle p(t)\middle| i\dot{\psi}(t) - \left(H_\lambda + \kappa|\psi(t)|^2\right)\psi(t)\right\rangle dt\right], \tag{3.2}$$

$H_\lambda = -\frac{1}{2m}\frac{\partial^2}{\partial x^2} + V(x,\lambda)$ is the single particle Hamiltonian which depends on the control parameter λ. The angle brackets denote the shorthand notation $\langle u|v\rangle = \int u^*(x)v(x)dx$ where u^* is the complex-conjugate of u. Note that $\hbar$ was set to 1.

$\delta L/\delta\psi$, $\delta L/\delta p$, $\delta L/\delta\lambda$ are called functional derivatives of the Lagrange functional $L(\psi,p,\lambda)$. They characterize the change of $L(\psi,p,\lambda)$ when one of the three parameters ψ, p, λ is varied. The point where all three derivatives become zero indicates a saddle point of the Lagrange function. This saddle point is exactly at the minimum of $J(\psi,\lambda)$, which indicates a minimum of the costs. Analytic calculation of these derivatives leads to the following set of equations:

$$i\dot{\psi} = \left(H_\lambda + \kappa|\psi|^2\right)\psi, \qquad \psi(0) = \psi_0, \tag{3.3a}$$

$$i\dot{p} = \left(H_\lambda + 2\kappa|\psi|^2\right)p + \kappa\psi^2 p^*, \qquad ip(T) = \psi(T) - \psi_d, \tag{3.3b}$$

$$\gamma\ddot{\lambda} = -\Re\mathfrak{e}\left\langle p\middle|\frac{\partial H_\lambda}{\partial\lambda}\middle|\psi\right\rangle, \qquad \lambda(0) = \lambda_0, \lambda(T) = \lambda_1. \tag{3.3c}$$

$\ddot{\lambda}$ is the second time derivative and λ_0, λ_1 are the initial and final control values at time $t = 0, t = T$. This set of equations consists of three different problems: (3.3a) is an initial value problem of the GPE. This equation is often called forward equation. It states that the system has to be in the initial state at the beginning of the manipulation. (3.3b) is a terminal value problem for the Lagrange multiplier p and is called adjoint equation. This equation states that the system has to be transferred to the desired state at the

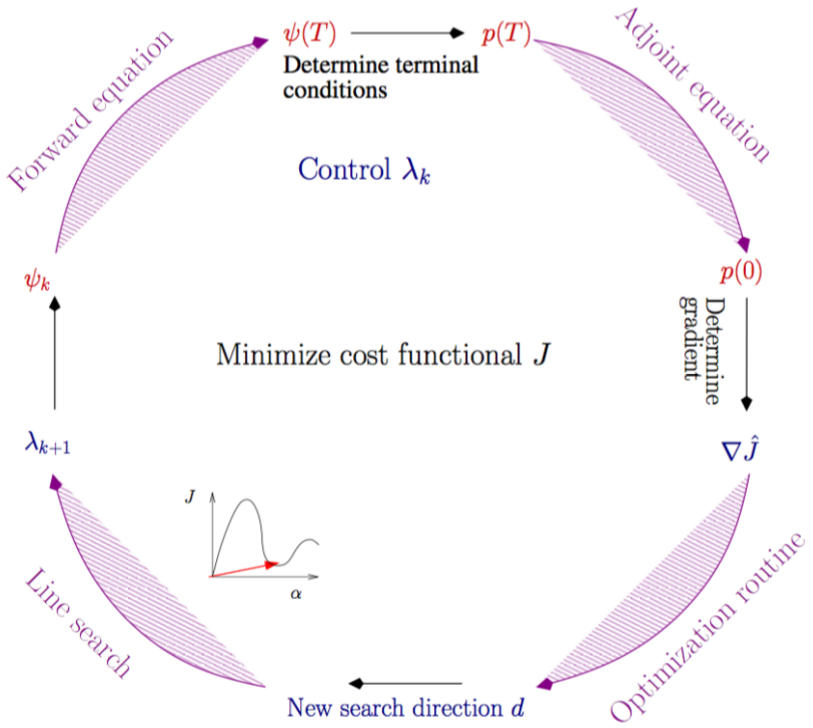

Figure 3.1: OCT operation scheme: One starts with a guess for the control λ_k. With this guess the adjoint equation is solved and a gradient is calculated. An optimization routine obtains a search direction for an improvement of the guess. A line search algorithm then determines an update for the guessed control λ_{k+1}. After this, the forward equation is solved and the iteration starts at the beginning. (source: [14]).

end of the manipulation at time T. (3.3c) is a boundary value problem that fixes the initial and terminal values and we refer to it as control equation. An effective control strategy is then given when all three equations (3.3a)-(3.3c) are fulfilled simultaneously.

It is possible to use this set of equations for an iterative calculation process. The key to this is to start with an initial guess of a control strategy and then obtain a more efficient strategy with every iteration step. How this is done within OCTBEC is explained in the following lines.

The iterative calculation scheme of OCTBEC is illustrated in figure 3.1. On the basis of this figure we explain the operation process for determining an efficient control strategy: To start the calculation, one has to provide an initial guess for the control λ_k (see top of figure). The guess of the control is used as a guide for the OCT routine. With λ_k as a guess the toolbox solves the *Forward equation* (3.3a) with the final state $\psi(T)$ (obtained by a simulation controlled by the guess) as solution. This equation is called forward, because it is solved forward in time. We can then obtain $p(T)$ from $\psi(T)$ and proceed with solving the *Adjoint equation* (3.3b). This equation is solved backwards in time and we get $p(0)$ as a result. If we have guessed a non-optimal control λ_k then

equation (3.3c) is no longer fulfilled. This means that $\delta L/\delta\lambda \neq 0$ respectively:

$$\frac{\delta L}{\delta \lambda} = -\gamma\ddot{\lambda} - \left\langle p \middle| \frac{\partial H_\lambda}{\partial \lambda} \middle| \psi \right\rangle. \tag{3.4}$$

(3.4) is called the gradient and we denote it as $\nabla_\lambda J$. From (3.4) it is possible to obtain a *search direction d* to improve the control strategy. Different methods for obtaining an appropriate *search direction d* are available, e.g. conjugate gradient method or BFGS. A detailed discussion about this methods would go beyond the scope of this thesis, but can be read in [15]. After determining a *search direction d* we have to decide how far we have to go along d. Therefore, a so-called *Line search* algorithm is used. This algorithm evaluates the costs for different step sizes along the previous defined *search direction d* to determine an optimal update for the next iteration. This procedure allows to update λ_k for an improved control strategy. After this, the optimization process starts again from the beginning with the updated control λ_{k+1}. This calculation loop is repeated as long as the norm of the derivation of the control $|\nabla_\lambda J|$ is greater than a user-defined parameter `tol`. The iterative calculation also stops if a predefined maximum number of iteration steps is reached.

To end this section, we discuss the unit system that is used by the toolbox: Length is measured in micrometers μm, time is measured in milliseconds ms and the reduced Planck constant was set to $\hbar = 1$. This is a convention that is used by the atom chip community. With this unit system, the unit of the interaction term is $[\kappa] = \text{ms}^{-1} = \text{kHz}$, which is the energy scale used by the toolbox. Because this community also prefers to use the frequency ν instead of the angular frequency ω, the interaction term is given by $\kappa = n\pi$ kHz, $n \in \mathbb{R}$.

More information about the OCTBEC toolbox and its operation method can be read in [16, 15].

3.3 `oct_split.m`

After the discussion of the basic operation principle of OCTBEC, we take a detailed look on the MATLAB file `oct_split.m`. The purpose of this script is to derive an efficient control strategy where a BEC is split from a single part into two separated parts. The manipulation is done by varying the confinement potential of the BEC. At the beginning of the manipulation the BEC is trapped by a harmonic oscillator potential. At the end of the manipulation the confinement potential takes the form of a double well potential. Both potentials are illustrated in figure 3.2.

Four exemplary results for different interaction terms κ, computed by `oct_split.m`, are shown in figure 3.3. This results were obtained by strategies that were optimized to split a BEC within $T = 10$ ms. The plots on the left side show the time evolution

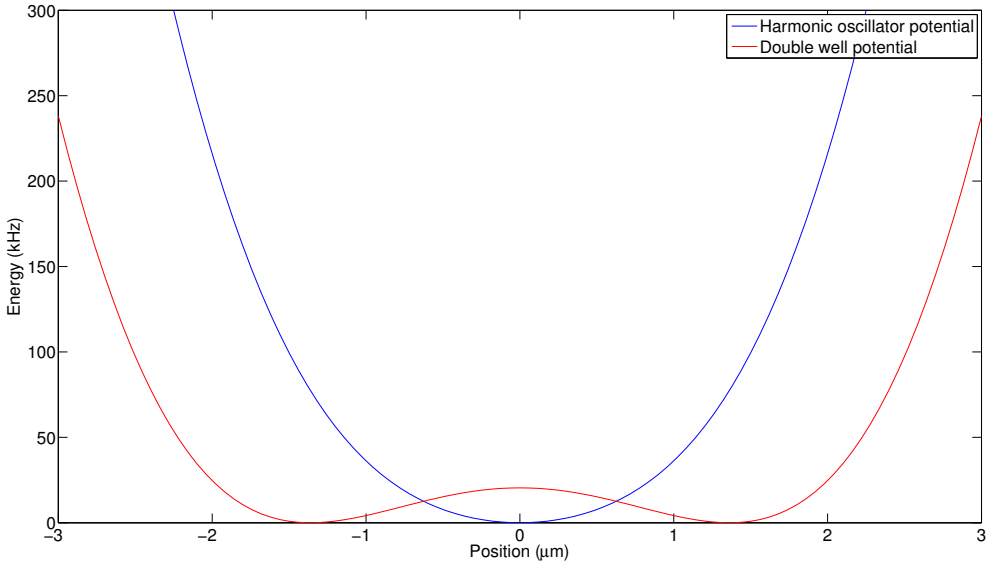

Figure 3.2: `oct_split.m` obtains a control strategy which varies the confinement potential for a BEC to achieve a splitting of the condensate into two parts. The initial confinement potential (blue) at time $t = 0$ is manipulated over time by the control parameter λ to a final potential (red) at $t = T$.

of the obtained control parameters $\lambda(t)$. Note that the function values of the control parameter $\lambda(0) = \lambda_0 = 0$ and $\lambda(T) = \lambda_1 = 1$ are the same for every calculation (required by the control equation (3.3c)). The function values $\lambda(0) = 0$ and $\lambda(T) = 1$ were chosen to fulfill the control equation (3.3c). The figures on the right show the time evolution of the density functions $|\psi(t)|^2$ within a time interval $[0, 20]$ ms. This figures are an arrangement of vertical slices of density functions at discrete points of the time interval. They show how the BEC behaves when it is manipulated by the obtained control strategy. The corresponding cost values $J(\psi(T))$ for the strategies of the figures in the right plots are listed in captions of the figures.

When analyzing this figures qualitatively, one can see that the control parameters of 3.3(a) - 3.3(c) look similar. More specifically, the control strategies of these three calculations look like a square root function. It has to be mentioned that the initial guess of the control parameter λ was actually made by using a square root function. What is striking is that the corresponding time evolutions of the density functions differ from one another. Comparing figure 3.3(a) and 3.3(b), one can see that the condensate is more closely packed in the potential minima for a noninteracting[1] condensate ($\kappa = 0$ kHz) compared to the repulsively interacting condensate ($\kappa = \pi$ kHz) (take care of the color bars when comparing both plots). The corresponding cost values for these two

[1] Actually, setting $\kappa = 0$ kHz results in an error message from the toolbox. To circumvent this, we set $\kappa =$ `eps` $\times \pi$. `eps` is called *Floating-point relative accuracy* and it is part of the `MATLAB` software. Its value is `eps = 2.2204e-16` and we assume that $\kappa =$ `eps` $\times \pi \approx 0$ kHz.

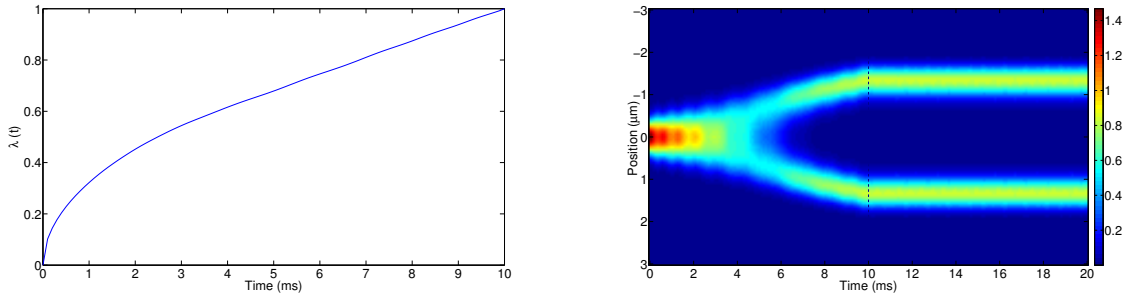

(a) $\kappa = \pi$, $J(\psi(T)) = 7.551 \times 10^{-4}$

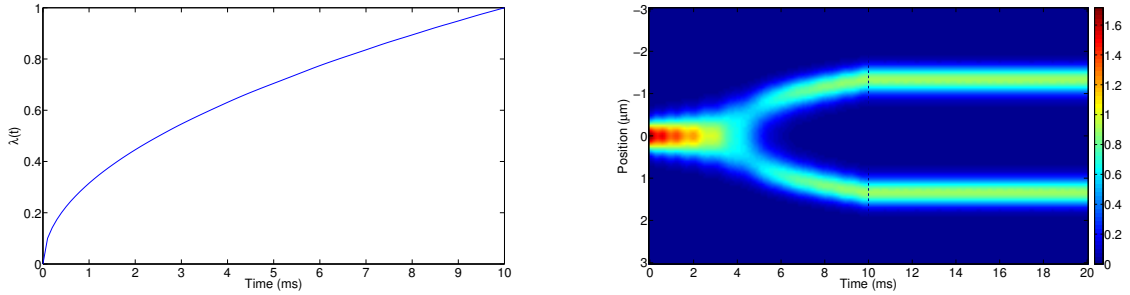

(b) $\kappa = 0$, $J(\psi(T)) = 7.122 \times 10^{-4}$

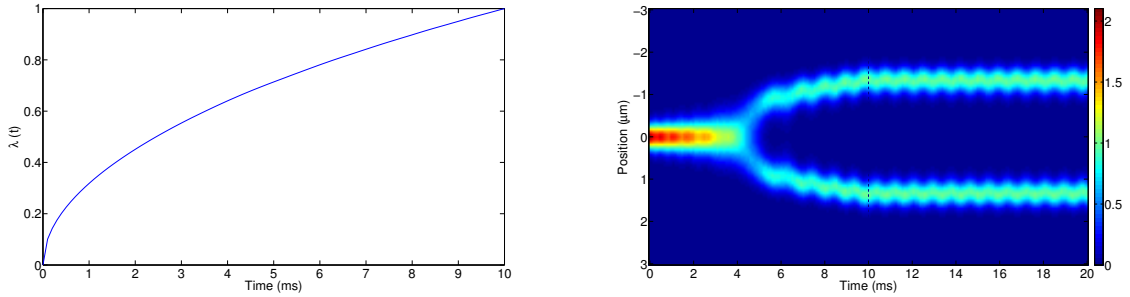

(c) $\kappa = -\pi$, $J(\psi(T)) = 2.528 \times 10^{-1}$

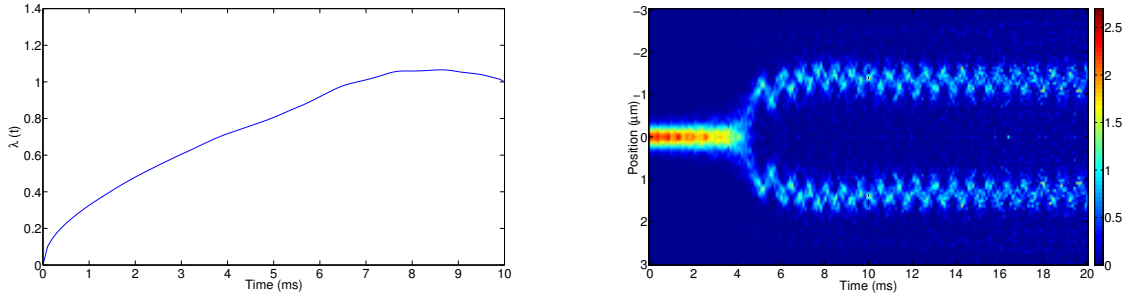

(d) $\kappa = -2\pi$, $J(\psi(T)) = 3.341 \times 10^{-1}$

Figure 3.3: Results of `oct_split.m` for splitting time $T = 10$ ms for different values of the nonlinearity κ: the figures on the left side show the evolution of the control parameter $\lambda(t)$; the figures on the right side show the density function $|\psi(t)|^2$ of the BEC controlled by the optimized confinement potential; $J(\psi(T))$ is the cost value of the corresponding desired state $\psi(T)$; all simulations were evaluated with the options `'timpr' = 10, 'mix' = 1e-2, 'tol' = 1e-4`; (source: this fiure was evaluated with `oct_split.m`)

calculations are of the order of 10^{-4}. This means that there is a mismatch between the desired and final state[2] of less than 0.1% (neglecting the influence of 'smoothness' of the control strategy). Generally speaking, costs of the order of 10^{-3} indicate that the control strategy is efficient. This is because such low costs mean that there is a mismatch between the final and desired state of less than 1%. Taking a closer look on figure 3.3(c) one observes a quite different time evolution of the density function compared with the ones from 3.3(a) and 3.3(b). It seems that after the manipulation is over, the condensate oscillates within the minima of the double well potential. When comparing the time evolution of the density function within the splitting process between those figures, one can recognize that the condensate already starts oscillating during the time interval $[0, 10]$ ms. The corresponding cost value $J(\psi(T))$ is of order 10^{-1} (10% mismatch) and therefore indicates an inefficient splitting process.

Last but not least, the obtained control strategy plotted in figure 3.3(d) shows a quite different behavior compared with the perviously discussed figures 3.3(a) - 3.3(c). Again, the start value as well as the final value of λ fulfill the control equation (3.3c). The control parameters for interactions of $\kappa = \pi, 0, -\pi$ kHz showed a monotonically increasing function. In contrast, the obtained control strategy of an attractive interacting condensate with $\kappa = -2\pi$ kHz is not a monotonic function. This means that at some points λ is greater than 1, which states that the desired double well potential is enlarged during the manipulation to achieve a splitting of the BEC. In principle, it does not matter how the control parameter develops over time as long as it does not vary in such a way that the costs are raised due to the second term in equation (3.3c). The belonging time evolution of the density function then shows a strong oscillation of the condensate. From this plot it is not possible to give a secure statement about the stability of the condensate. This means that we cannot say whether the condensate will only oscillate within the potential or if it will vanish due to the strong oscillation. To give a more justified answer about this, further calculations will be required. The corresponding cost value $J(\psi(T))$ is of order 10^{-1} (10% mismatch) just like the cost value belonging to figure 3.3(c) and thus indicates an inefficient splitting process.

When summarizing these observations, it follows that the OCTBEC toolbox derives suitable strategies for a splitting of BECs where interactions of $\kappa = 0, \pi$ kHz are present. It has to be mentioned that all these results were determined with the default settings. In the case of $\kappa = -\pi, -2\pi$ kHz the condensate was manipulated in a way that it oscillates when the manipulation is over. The corresponding cost values for these cases indicated that these strategies are not efficient. The question now is, if it is possible to modify the toolbox settings to obtain efficient strategies for these cases. If this is possible, then an investigation of these efficient splitting processes should be made. In the following chapters we analyse the `oct_split.m` script in more detail.

[2]The desired state is not the same as the state at $t = 10$ ms of the color plot. The difference between them is that the desired state is used as an input for the derivation of the control strategy and cannot be changed. The state at $t = 10$ ms is results of the simulation of the BEC with the derived strategy.

Chapter 4

Investigation method

As the results from chapter 3 showed, the toolbox OCTBEC does not derive efficient control strategies for attractive interactions ($\kappa < 0$ kHz) in a BEC. The task in this chapter is to analyze the OCTBEC toolbox in more detail and to introduce a method which allows us to obtain the reasons for failure of the optimization routine. It has to be mentioned that the failure of the routine does not mean that the toolbox derives inappropriate solutions due to a wrong description of the BEC nor an incorrect implementation of the OCT scheme. What is more likely is that the input parameters and settings have to be changed for values of $\kappa < 0$ kHz.

In this chapter we create a list of aspects that have to be checked when investigating the calculation results. The following text is structured like this: Section 4.1 deals with the calculation routine that derives the initial and desired states, which define the starting situation for the optimization problem. In section 4.2 we introduce a quantity that allows to characterize the behavior of BECs during the splitting process in more detail. At the end of this chapter, an extension of the iterative calculation scheme is discussed in section 4.3.

4.1 Initial and desired states

Before OCTBEC can start with the iterative optimization calculations, several parameters and options have to be set. Among other parameters the initial and desired states are one of the most important inputs for the optimization process. If this states do not represent the starting situation of the inverse problem correctly, no appropriate solution can be expected. To make this clear, think about the previously discussed problem of the production process of a company. If one performs optimization calculations for a strategy that do not take resources into account that are required for the goods, a suitable result cannot be expected. The same also applies for the optimization of a splitting process. It should be clear that if the desired state of a BEC does not represent a split condensate correctly, it is impossible to derive an efficient strategy for such a manipulation. It follows that it should be the first task to check if the states are correct when investigating the results. The required characteristics for the initial and desired

states are explained in chapter 5 when the actual analyzation is done. We do so, because an explanation with the aid of an example gives a better understanding than a formal description.

But what has to be done if it turns out that improper states were used for the optimization calculation? The actual calculation of the initial and desired states is done by the custom toolbox function `groundstate`. This function computes the Gross-Pitaevskii ground state using the optimal damping algorithm from [17]. As mentioned in reference [16], the calculation of desired states (ground states within double well potentials) sometimes fails. It is then recommended to use a different calculation method by using the `mix` parameter to circumvent this problem. This means that if improper states are observed the desired states have to be recalculated with an additional or improved `mix` option and the whole optimization calculation has to be repeated with the corrected states.

In the following chapter, where the analysis of the results is done, the initial and desired states are checked. If it turns out that improper states were used for the calculations, the states are recalculated with a modified `mix` option and the optimization calculation is repeated. This should exclude a source of error that can lead to inefficient control strategies.

4.2 Oscillation of density function

As already discussed, the evolution of the density functions showed oscillations in figure 3.3 for the cases of $\kappa = -\pi, -2\pi$ kHz. These plots make it difficult to determine how strong the oscillations of the condensates are, because of the presentation of these results as color plots. To circumvent this problem, we take a look at the uncertainty in position of the condensate.

In principle, the uncertainty of a quantity x is defined by

$$\sigma = \sqrt{var(x)} = \sqrt{\langle x^2 \rangle - \langle x \rangle^2}, \tag{4.1}$$

$var(x)$ is the variance of the observable x, $\langle x \rangle$ and $\langle x^2 \rangle$ are the expectation values of x and respectively x^2. The standard deviation σ describes how close the data points x are packed to the mean value $\langle x \rangle$. Small values of σ indicate that the data points are closely packed around $\langle x \rangle$, while a high standard deviation indicates that the data points are spread out wider around $\langle x \rangle$.

The expectation value of the position operator $\hat{Q}$ can be calculated by

$$\langle \hat{Q} \rangle = \int_{-\infty}^{\infty} \langle \psi | x \rangle \, \hat{Q} \, \langle x | \psi \rangle \, dx = \int_{-\infty}^{\infty} x |\psi(x)|^2 dx, \tag{4.2}$$

and the expectation value of $\hat{Q}^2$ by

$$\langle \hat{Q}^2 \rangle = \int_{\infty}^{\infty} \langle \psi | x \rangle \, \hat{Q}^2 \, \langle x | \psi \rangle \, dx = \int_{-\infty}^{\infty} x^2 |\psi(x)|^2 dx. \tag{4.3}$$

Those equations are valid if the wave function ψ is given in position-space, because then the representation of the position operator simply is $\hat{Q} = x$. The uncertainty in position is then given by

$$\sigma = \sqrt{\langle \hat{Q}^2 \rangle - \langle \hat{Q} \rangle^2}. \tag{4.4}$$

When analyzing the results in the following chapter we calculate the uncertainty in position for every time step of the corresponding time evolutions of the BEC. σ together with the color plots of the time evolution of the BEC then enables to give a more justified answer about the behavior of a BEC during and after the manipulation is finished. A detailed explanation of the actual meaning of this quantity is given when analyzing the results in chapter 5.

4.3 Extending iterative calculations

In section 4.1 we found out that the solutions for the initial and desired ground state of the BEC, that are passed on to the OCT routine, have to be checked in order to exclude one source of error. Let us assume that these parameters are correct but the toolbox still derives control strategies with cost values greater than 10^{-3} (greater mismatch than $0,1\%$). What could be the reason for the derivation of such inefficient control strategies?

To answer this question, we have to take a look back on the basic properties of the OCT routine presented in chapter 3. In section 3.1 we discussed the operation scheme of an OCT loop where at some point the gradient of the cost function ∇J was introduced. This quantity gives information about the search direction to determine the minimum of the cost functional $J(\psi(T))$. Applying a search line algorithm on this quantity gives a step size for updating the control parameter in the next iterative calculation step. As we know, the iteration process terminates if the maximum number of iteration steps is reached. The maximum number of iterations used for the calculations of the results from 3.3 was set to 10. What if the OCT routine would need more than 10 iteration steps to derive an efficient strategy? This aspect was not considered during all the calculations that were perviously done. Due to this, we modified the toolbox in a way that the optimization calculations are extended. This was done by increasing the maximum number of iteration steps to 30. To prevent a termination before the maximum number of iterative steps is reached, the `tol` parameter had to be removed.

The actual investigation in the following chapter uses this extension of the OCT routine. In addition to this, the cost function $J(\psi, \lambda)$ is then monitored during the optimization calculations. From this data it should be able to see how the costs develop during the optimization. In addition, it should be possible to recognize if there is room left for further improvements on the strategies or not.

Chapter 5

Results

To start this chapter, we shortly summarize the investigation aspects:

- First, we analyze the initial and desired ground states that are used as inputs for the OCT routine. Therefore we discuss the shape of the density functions, the arrangement of the density functions compared to the confinement potential and the corresponding uncertainties for this states. If there are states that do not match the criteria for a valuable input, the calculation of them has to be repeated with a modified `'mix'` option. Otherwise it is difficult to derive an efficient control strategy.

- Another aspect that is considered in this analysis is the evolution of the density function that results from the obtained control strategies. We discuss the behavior of the condensates during and after the manipulation process. In addition we have calculated the evolutions of the uncertainty of the condensate that belongs to the density functions. From this we should be able to give a more justified answer about oscillations of a BEC after a splitting process is finished.

- Because we have extended our iteration process by increasing the number of maximum iteration steps, we also monitored the costs for each iteration step. With this information it should be possible to estimate if the OCT routine converges to a cost value that characterizes an efficient splitting process. This results are presented in a figure together with a comparison between the initial guess and the final control strategy. This should give us a more justified answer about the efficiency of the control strategies.

All results and figures that follow in this chapter were obtained with the `oct_split.m` program, where the maximum number of iteration steps was increased from 10 to 30. In addition to this, we have removed the termination condition $|\nabla_\lambda J| <$ `tol`. This modifications allows us to extend the iterative calculations to investigate if the costs converge after 30 iteration steps. We used the same options as for the calculations of the results presented in figure 3.3 (`timpr = 10, mix = 1e-2, tol = 1e-4`). If we use other options or settings, we clearly mark this.

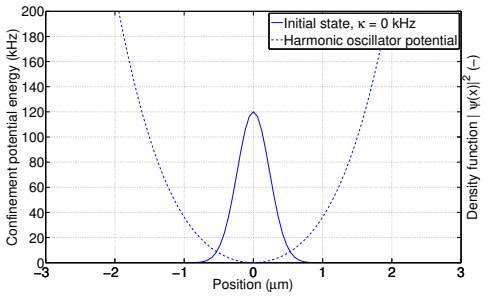

(a) Initial state density function and harmonic oscillator potential at $t = 0$ ms. Uncertainty in position: $\sigma_{\kappa=0}^{\text{initial}} = 0.230$ μm.

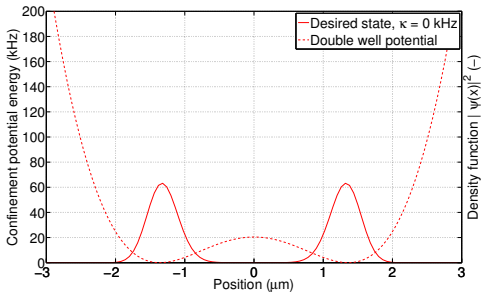

(b) Desired state density function and double well potential at $t = 10$ ms. Uncertainty in position: $\sigma_{\kappa=0}^{\text{desired}} = 1.323$ μm.

Figure 5.1: Initial and desired states together with the belonging potentials with atom-atom interaction $\kappa = 0$ kHz.

We have structured this chapter like this: Section 5.1 deals with the analysis of a non-interacting BEC where $\kappa = 0$ kHz. In section 5.2 we analyze results with attractive interactions $\kappa = -\pi$ kHz. After this, we discuss a BEC where $\kappa = -2\pi$ kHz was set. All these analysis are related to the results that were presented in section 3.2.

5.1 No interactions: $\kappa = 0$ kHz

Before we start with the analysis of a non-interacting BEC we review the observations from figure 3.3(b): The obtained control strategy $\lambda(t)$ for this case looks almost like a square root function, which is a steady increasing function. The corresponding cost value $J(\psi(T))$ is about 7×10^{-4}, which indicates an efficient splitting process. The time evolution of the density function showed that the condensate is split into two parts by this control strategy. In addition, no significant oscillations after the manipulation can be recognized from the color plot.

The first aspect that is discussed in this section deals with the initial and desired states that were passed on to the OCT routine. Therefore we have taken the states that were used for the calculations of the results presented in figure 3.3(b). We have plotted the density functions of these states in figure 5.1 together with the potentials. The uncertainties in position $\sigma_{\kappa=0}$ are listed in the corresponding captions.

What do this states tell us about a non-interacting BEC at the beginning and at the end of the manipulation? The shape of the initial state is that of a Gaussian. It is centered around the minimum of the harmonic oscillator potential, which is at $x = 0$ μm. This shape and arrangement of the state is what we expect, because this is the analytical solution for a condensate that is confined in a single well potential (see section 2.4). This means that the initial state was determined correctly. In contrast, the desired state is represented as a wave package that consists out of two Gaussians. Each of the sub-Gaussians is centered at one minimum of the double well potential. The physical

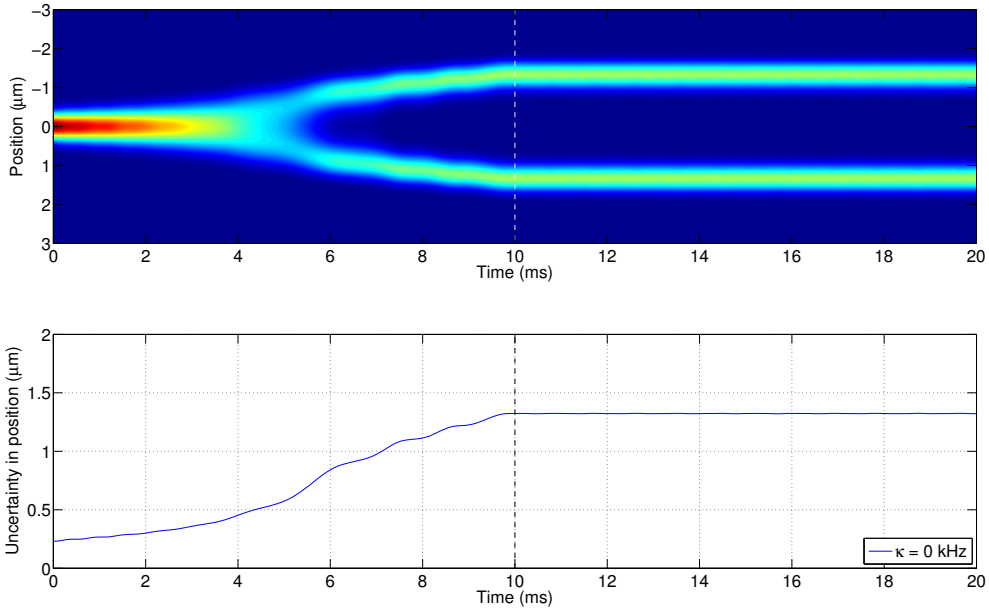

Figure 5.2: Top plot shows the time evolution of the condensate that was simulated with the control strategy obtained with the extended calculation. Bottom plot shows the development of the uncertainty in position that belongs to the upper plot.

interpretation of this is that a particle of the BEC is equally likely to be met around both potential minima. In contrast, the probability to meet a particle around the origin $x = 0$ μm is zero, because at this point the potential is higher compared to the minima. This means that the BEC in its ground state avoids to appear at the origin. This aspect is what is required for a ground state of a split condensate. From this it follows that the desired state can also be used as a valuable parameter, because it correctly represents a split condensate.

What additional information can be extracted from the uncertainties of position? We have listed the numerical values of $\sigma_{\kappa=0}$ in the corresponding captions of the plots. The values are $\sigma_{\kappa=0}^{\text{initial}} = 0.230$ μm and $\sigma_{\kappa=0}^{\text{desired}} = 1.323$ μm. Remember, the uncertainty characterizes the packing of atoms around the mean position $\langle x \rangle = 0$ μm[1]. Since the desired state describes a condensate that avoids to appear around the origin, the packing of the BEC around $x = 0$ μm is smaller compared to the initial state. This is also reflected by the values of $\sigma_{\kappa=0}$, because $\sigma_{\kappa=0}^{\text{initial}} < \sigma_{\kappa}^{\text{desired}}$. The question is now, how do the uncertainties $\sigma_{\kappa}^{\text{initial}}, \sigma_{\kappa}^{\text{desired}}$ change if the atom-atom interaction κ is modified? To answer this we are going to use the initial and desired states as well as the corresponding uncertainties in the following sections as a reference.

The next aspect we consider is the time evolution of the BEC that is modified by the

[1] $\langle x \rangle = 0$ μm is obvious, because both states are symmetric around the origin $x = 0$ μm.

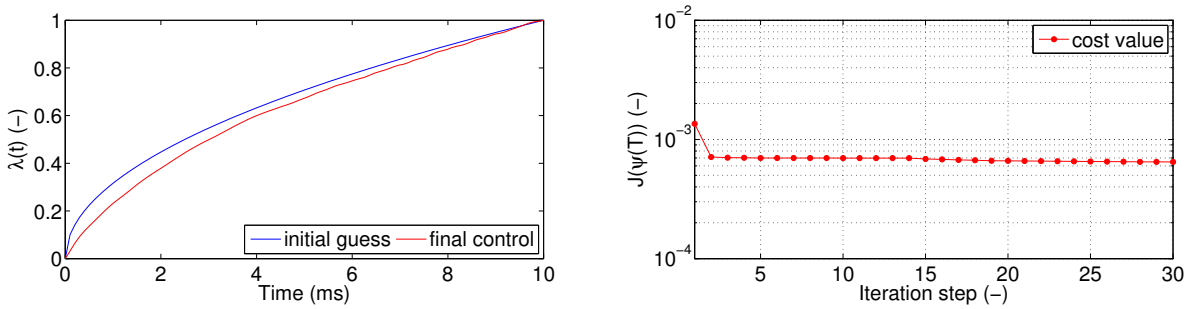

Figure 5.3: The left figure contains the initial guess control strategy (blue line) and the final control strategy (red line). The right figure shows the development of the costs $J(\psi(T))$. This results were obtained for a BEC with $\kappa = 0$ kHz.

obtained control strategy. Therefore we take a look at figure 5.2 which consists of two plots. The top plot shows the evolution of the density function. It consists of vertical slices that represent the density function for each time step t. This plot represents the manipulation by the control strategy that was obtained after 30 iteration steps. The bottom plot in figure 5.2 shows the evolution of the uncertainty in position. This chart is constructed by values of $\sigma_{\kappa=0}$, were each value at time t belongs to the density function at time t from the top plot. The uncertainty itself was calculated by equation 4.1.

What does this figure tell us about the evolution of the condensate? The first thing we see is that the condensate is clearly split into two separated parts. This means that the corresponding control strategy is definitely applicable for a splitting process. If we take a detailed look at the manipulation, which takes place within $[0, 10]$ ms, then we see that the condensate is steadily pulled apart until it reaches the final state. The evolution of $\sigma_{\kappa=0}$ also rises steadily during the manipulation, which indicates that the packing density around the origin decreases during the manipulation. This matches with the uncertainties that were calculated for the initial and desired states.

The evolution of the density function in the time interval $[10, 20]$ ms shows the behavior of the condensate when the manipulation is stopped. A color plot makes it hard to recognize small changes of a density function, but the evolution of σ_κ lets us recognize such variations. As one can see from the top plot the condensate does not change its shape when the manipulation is over. However, the corresponding evolution of $\sigma_{\kappa=0}$ also remains constant, which means that the condensate is truly stable after the manipulation is finished. It follows, that this strategy manipulates the condensate in a way that it is split and remains constant afterwards.

The last aspect that is discussed in this section deals with the control strategy and the cost functional $J(\psi(T))$. This parameters are presented in figure 5.3. The plot on the left side contains the initially guessed and the final control strategy. A history of the cost values that belong to the derivation of the final control strategy is presented in the right plot. This figure should serve as a check for the calculation process. Especially the development of the costs should let us determine whether the costs converge to a

minimum or if there is room left for further improvements on the strategy.

Starting with the plot on the left one sees that the final control has almost the same shape as the initially guessed strategy. The final strategy was determined after 30 iterations, which means that the initial guess was made quite good. If the initial strategy would not have been a good guess, the OCT routine would have derived a significantly different looking strategy to lower the costs. The good guess of the initial strategy is also confirmed by the right plot. It shows that the costs were reduced within two iteration steps to a value of about 6×10^{-4}. The OCT routine was not able to lower the costs even more within the remaining iterations. The cost value at the 30th iteration step is almost equal to the cost value from the 2nd iteration step. However, costs of the order of 10^{-4} already indicate that the match of the final and desired state is very good. This means that further improvement on this strategy would not significantly improve the final control strategy and is therefore not necessary.

To end this first analysis we shortly summarize the observations that were made in this section: The initial and desired states represent our starting situation of the optimization problem correctly. The strategy that was derived with the extended calculation is able to split the condensate. This was no surprise, because the result from figure 3.3(b) was already an efficient manipulation. The evolution of the uncertainty confirmed the statement about the stability of the condensate when the manipulation is over. The development of the costs showed that the derived strategy is truly valuable for a split manipulation. In addition, we found out that the initial guess was made well, because the costs approach a small value after two iterations. Further improvements on this control strategy are not required, because the discussed results represent a good manipulation for a BEC where no atom-atom interactions are present.

In the following sections we use the figures and the results that were analyzed in this section as a reference. A comparison with these results should give us information about how the interatomic interaction κ influences the manipulation of a BEC as well as the optimization calculations for attractive interactions.

5.2 Attractive interactions: $\kappa = -\pi$ kHz

This section deals with a BEC where attractive interactions with $\kappa = -\pi$ kHz are present. The results from figure 3.3(c) showed that it is possible to derive a strategy that splits the condensate. The strategy looks similar to the strategies that were derived for the cases of $\kappa = \pi, 0$ kHz. The evolution of the density function showed that the BEC clearly oscillates when the manipulation is over. The final cost value was on the order of 10^{-1} which indicates that the derived strategy is inefficient. The following analysis follows the same scheme as in the previous section. In addition, the results of this section are compared with the references that were presented previously.

To start this section we discuss the initial and desired states that were used for the calculations of the results from figure 3.3(c). The states for the case of $\kappa = -\pi$ kHz

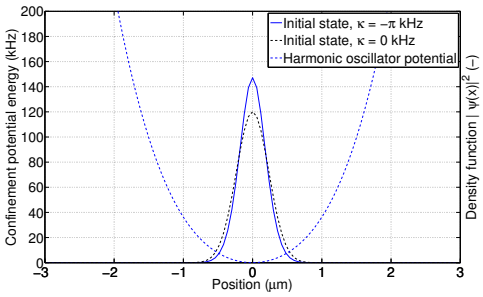

(a) Initial state density function and harmonic oscillator potential at $t = 0$ ms. Uncertainty in position: $\sigma^{\text{initial}}_{\kappa=-\pi} = 0.196$ μm, $\sigma^{\text{initial}}_{\kappa=0} = 0.230$ μm.

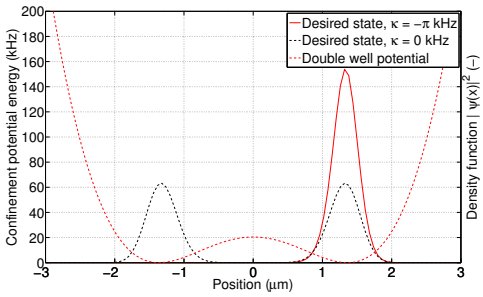

(b) Desired state density function and double well potential at $t = 10$ ms. Uncertainty in position: $\sigma^{\text{desired}}_{\kappa=-\pi} = 0.229$ μm, $\sigma^{\text{desired}}_{\kappa=0} = 1.323$ μm.

Figure 5.4: Initial and desired states together with the corresponding potentials with atom-atom interaction $\kappa = -\pi$ kHz. The solid lines represent the density functions for $\kappa = -\pi$ kHz and the black dashed lines represent the reference states ($\kappa = 0$ kHz) from figure 5.1;

are presented in figure 5.4 together with the corresponding potentials and the reference states. The uncertainties in position are listed in the corresponding captions of the subfigures.

When investigating this figure one thing strikes immediately: the desired state (solid red line) presented in 5.4(b) has a significantly different shape than the reference state (black dashed line). In more detail, the desired state is an ordinary Gaussian that looks similar to the initial state. The probability distribution is zero around the left potential minima and non-zero around the other minima. The physical interpretation of this is that a particle of the condensate can only be met around the right potential minima. A condensate that is described by such a density function is a single cluster of atoms. Since we require that the desired state has to be a split condensate, this state can obviously not be used for the calculations.

The relative high cost value that was obtained for the result from figure 3.3(a) has to do with this incorrect desired state. Remember, the first term of the cost functional (3.1) rates the difference between the desired and the final state. As the evolution of the density function showed, the condensate is split into two separate parts. This means that the final state at $t = 10$ ms looks similar to the reference state presented in figure 5.4(b). It should be clear that this difference was responsible for the high costs. It has to be mentioned that an extension of the calculation with this desired state would not have improved the costs and therefore the strategy. The reason for this is that the toolbox varies the strategy in a way that the final state matches the desired state as good as possible. This means that an extended calculation would have made the result even worse.

At this point a discussion about the initial state is left out. We did so, because we found out that this set of states cannot be used as an input for an optimization

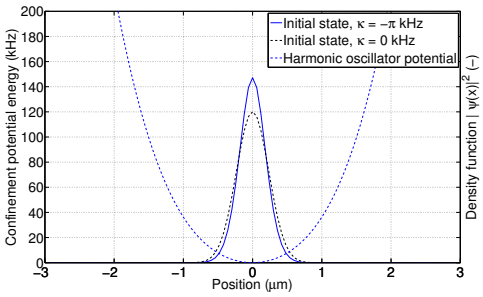

(a) Initial state density function and harmonic oscillator potential at $t = 0$ ms. Uncertainty in position: $\sigma^{\text{initial}}_{\kappa=-\pi} = 0.196$ μm, $\sigma^{\text{initial}}_{\kappa=0} = 0.230$ μm.

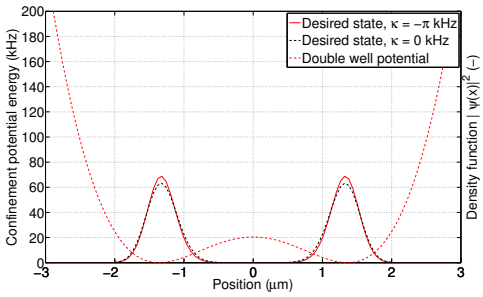

(b) Desired state density function and double well potential at $t = 10$ ms. Uncertainty in position: $\sigma^{\text{desired}}_{\kappa=-\pi} = 1.327$ μm, $\sigma^{\text{desired}}_{\kappa=0} = 1.323$ μm.

Figure 5.5: Initial and desired states together with the corresponding potentials with atom-atom interaction $\kappa = -\pi$ kHz. The solid lines represent the density functions for $\kappa = -\pi$ kHz and the black dashed lines represent the reference states ($\kappa = 0$ kHz) from figure 5.1. These results were obtained with modified option `mix = 1e-5`.

calculation. These states have to be recalculated with modified options for further investigations. Also a discussion about the uncertainties $\sigma_{\kappa=-\pi}$ is irrelevant, since the state are no valuable inputs.

Because the set of states discussed previously is not applicable as an input we have recalculated these states with modified options. Figure 5.5 contains the results that were obtained by calculations where the `mix` parameter was changed from `1e-2` to `1e-5`. How did the states change?

At first glance both states have the same shape as the reference states (black dashed lines). The Gaussian of the initial state is the predicted solution to the problem in a harmonic oscillator potential. The combination of two sub-Gaussian in the desired state fulfills the physical aspects to represent a split condensate. Obviously, this set of states represents the starting situation of the split problem qualitatively correct.

But how do these states differ from the reference states? Starting with figure 5.5(a) we see that the peak of the initial state is much higher than the peak of the reference state. It holds that the area under a probability distribution is conserved as 1. This means that if the peak of a Gaussian gets higher the width of the curve has to get smaller. As we know the width of a Gaussian is characterized by its standard deviation, which we called σ_κ. The values of the uncertainties of the states presented in this figure are $\sigma^{\text{initial}}_{\kappa=0} = 0.230$ μm and $\sigma^{\text{initial}}_{\kappa=-\pi} = 0.196$ μm. This means that the width of the initial state is smaller compared to the width of the reference state. Due to the definition of σ_κ a smaller width of the density function corresponds to a higher packing density of the condensate. It follows that the packing density of the initial state is higher than for the reference state. In other words, a condensate where attractive interactions are present is tighter packed than a BEC without atomic interactions. This aspect was already

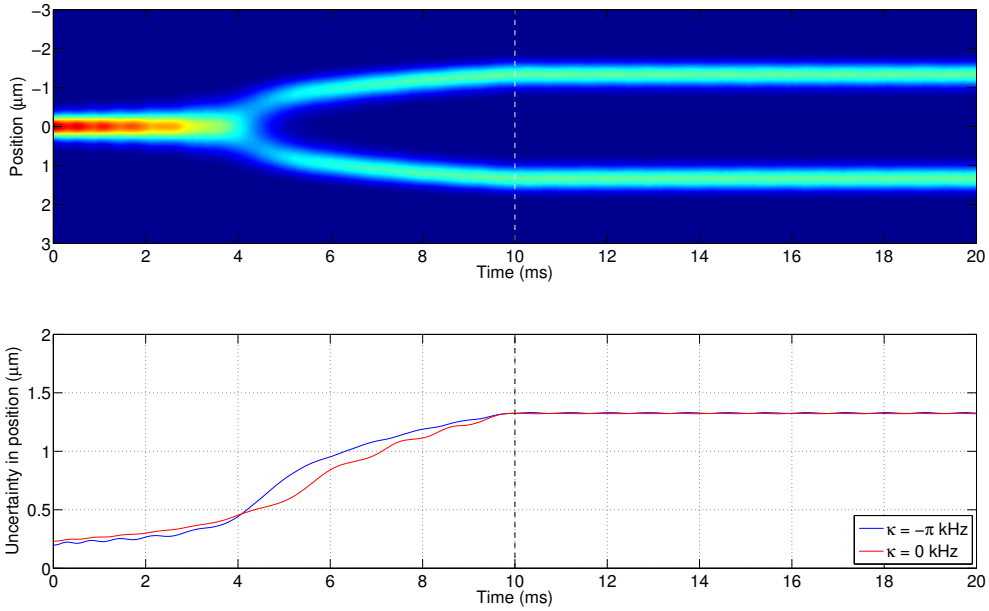

Figure 5.6: Top plot shows the time evolution of the condensate that was simulated with the control strategy obtained with the extended calculation. Bottom plot shows the development of the uncertainty in position that belongs to the upper plot (solid blue line) as well as the development of the uncertainty from a BEC with $\kappa = 0$ kHz from figure 5.2, which serves as a reference (solid red line).

discussed in section 2.4 and is correctly reflected by this result.

The situation is different when we consider the desired states. The problem is that the desired states are wave packages that consist of two Gaussians. As we know, the uncertainty in position rates the variation around the mean position, which is $\langle x \rangle = 0$ μm. This means that $\sigma_\kappa^{\text{desired}}$ does not give a numerical answer about the packing density within one cluster of the condensate. This quantity only tells us how wide the density function is spread out around $\langle x \rangle$. The values of the uncertainty are $\sigma_{\kappa=0}^{\text{desired}} = 1.323$ μm and $\sigma_{\kappa=-\pi}^{\text{desired}} = 1.327$ μm. It follows that $\sigma_{\kappa=0}^{\text{desired}} < \sigma_{\kappa=-\pi}^{\text{desired}}$. This means that the particles of a BEC where $\kappa = -\pi$ kHz are more spread out around the origin compared to a BEC with no interactions. Although $\sigma_\kappa^{\text{desired}}$ does not give information about the packing density within one cluster, it is possible to analyze this qualitatively. Consider only one part of the desired state (e.g. the left sub-Gaussian). This sub-Gaussian looks similar to the initial state. When we assume that the area under this sub-Gaussians is conserved as 1, then the same arguments about the packing density of the initial states also apply for this part of the density function. This means that each part of a split condensate where $\kappa = -\pi$ kHz is tighter packed than each cluster of a split BEC where $\kappa = 0$ kHz.

In the previous lines we have analyzed an issue that influences the derivation of a

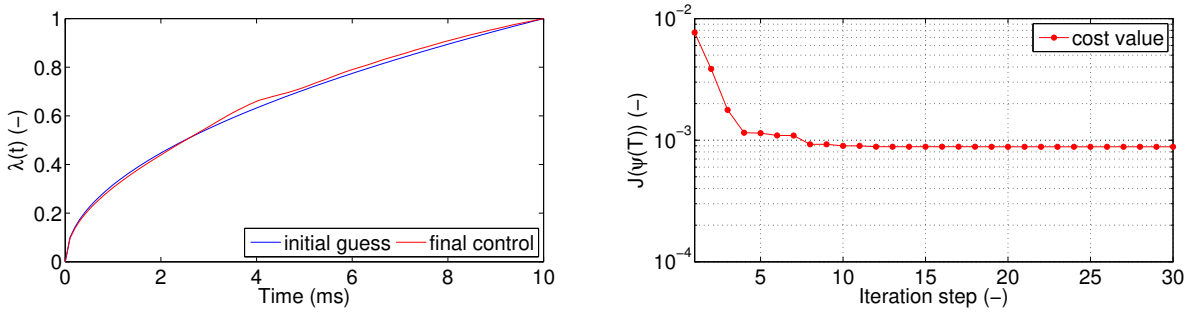

Figure 5.7: The left figure contains the initial guess control strategy (blue line) and the final control strategy (red line). The right figure shows the development of the costs $J(\psi(T))$. This results were obtained for a BEC with $\kappa = -\pi$ kHz.

control strategy. By modifying the calculation of the inputs, we have resolved this issue. Here follows the analysis of a control strategy that was derived with the corrected states. Figure 5.6 contains the evolution of the density function in the top plot and the development of the corresponding uncertainty in the bottom plot. In addition, we have added the evolution of the uncertainty from 5.2 which should serve as a reference.

Starting with the top plot one sees that the condensate is clearly split into two separated parts. After the manipulation is over no visible changes of the condensate can be seen within the time interval $[10, 20]$ ms. This is a quite contrary result compared to the result that was presented in figure 3.3, where variations of the condensate were present after the manipulation was finished.

A comparison between the uncertainty that belongs to the top plot and the reference uncertainty shows that there is a difference between them. At the beginning of the manipulation both uncertainties develop almost in the same way. At about $t = 4$ ms $\sigma_{\kappa=-\pi}$ starts to increase stronger than $\sigma_{\kappa=0}$. This earlier increase of $\sigma_{\kappa=-\pi}$ is related with the actual split of the BEC, which takes place at about $t = 4$ ms [2]. The splitting for the BEC with $\kappa = 0$ kHz happens at about $t = 5$ ms (see figure 5.2). This means that the condensate with $\kappa = -\pi$ kHz is split earlier than the reference condensate. But this will not be the general case, because there may exist strategies that modify BECs in different ways where the split occurs after the reference condensate is split. Nevertheless, at the end of the manipulation the uncertainties take almost the same value. When taking a detailed look at $\sigma_{\kappa=-\pi}$ kHz in the time interval $[10, 20]$ ms one can see that $\sigma_{\kappa=-\pi}$ oscillates with a very small amplitude. Obviously, this oscillation is so small that it was impossible to be seen in the evolution of the density function. Further it can be stated that the condensate will not change its shape drastically due to this oscillation.

Last but not least the analysis of the control strategy and the development of the costs follows. Figure 5.7 contains the final control strategy in the left plot and the history of the costs is presented in the right plot.

[2] It is hard to determine when the split exactly happens, because the density functions changes continuously during this process.

As one can see the final control strategy is almost the same as the initially guessed strategy. This means that it was not necessary to change the guessed strategy significantly to obtain a split of the condensate. The history of the costs then tells that the costs are lowered within about 4 iterations down to a value of about 1×10^{-3}. In the following iterations the toolbox was able to decrease the costs even further. As one can see after the 10th iteration step the costs do not change anymore. This lets us assume that the costs converge at this point to a final value of about $J(\psi(T)) \approx 9 \times 10^{-4}$. This low costs together with the previously discussed evolution of the states indicates that this strategy is truly an efficient one. Comparing the costs from the result where improper states were used (figure 3.3(c)) with the costs of the corrected strategy, one can see that the correction of the states was a good improvement. Again, it turned out that the initially guessed strategy is a good guess for the optimization.

Before continuing with the next analysis, a short summary about the investigated aspects from this section follows: The investigation of the initial and desired states showed that the states used for the calculation of the results 3.3(c) did not correctly represent the starting situation of the split problem. This required a recalculation of states, which was done by modifying the `mix` option. An optimization with the corrected states provided a significantly different result of the behavior of the BEC. This strategy also splits the condensate successfully, but the oscillations after the manipulation were significantly reduced. The cost value that corresponds to this new strategy is smaller than 10^{-3} which characterizes this strategy as an efficient one.

5.3 Attractive interactions: $\kappa = -2\pi$ kHz

The last section of this chapter deals with the analysis of a BEC where attractive interactions with $\kappa = -2\pi$ kHz are present. The first result for this case presented in figure 3.3(d) showed that the derived strategy is totally different compared to the ones that were derived for the cases of $\kappa = 0, \pi, -\pi$ kHz. The evolution of the density function showed that the condensate is split. When the manipulation is over the BEC shows strong oscillations. It was not possible to determine if the condensate will totally spread out and therefore be lost or not. In addition, the corresponding cost value was $J(\psi(T)) \approx 3.3 \times 10^{-1}$ which indicates that this strategy was not efficient.

A note about the following analysis of the results has to be given here: The toolbox seems to be unstable if one tries to extend the iteration process. The routine sometimes terminates the calculation and throws an error that has to do with a failure of the optimization routine. This failure appears randomly and a quick search for the source of this error did not lead to a solution. Furthermore, the results cannot exactly be reproduced by trying to execute the toolbox a few times. Either the toolbox terminates the calculation or the obtained costs and density functions are different compared to pervious calculations. The toolbox derived two control strategies that manipulate BECs in significant different ways. We are going to discuss both results in this section.

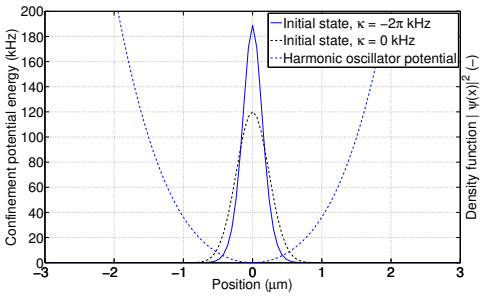

(a) Initial state density function and harmonic oscillator potential at $t = 0$ ms. Uncertainty in position: $\sigma^{\text{initial}}_{\kappa=-2\pi} = 0.159$ μm, $\sigma^{\text{initial}}_{\kappa=0} = 0.230$ μm.

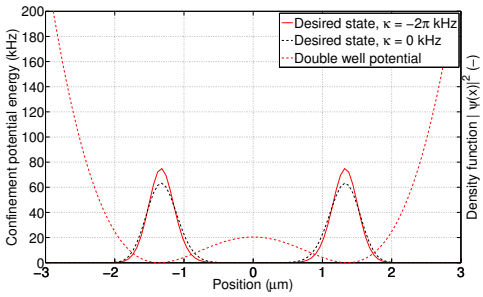

(b) Desired state density function and double well potential at $t = 10$ ms. Uncertainty in position: $\sigma^{\text{desired}}_{\kappa=-2\pi} = 1.329$ μm, $\sigma^{\text{desired}}_{\kappa=0} = 1.323$ μm.

Figure 5.8: Initial and desired states together with the corresponding potentials with atom-atom interaction $\kappa = -2\pi$ kHz. The solid lines represent the density functions for $\kappa = -2\pi$ kHz and the black dashed lines represent the reference states ($\kappa = 0$ kHz) from figure 5.1. This results were obtained with modified option `mix = 1e-5`.

As we did in the previous sections we start with the discussion about the initial and desired states. The states that were used for the derivation of the first result for $\kappa = -2\pi$ kHz (figure 3.3(d)) looked similar to the improper states that were presented previously in figure 5.4. In more detail, the desired state did not represent a particle that is equally likely to be met around both potential minima. Because a detailed discussion about this issue was already given, a presentation of the improper states for $\kappa = -2\pi$ kHz is left out. Again, it is required to recalculate the states with a modified `mix` option. Figure 5.8 contains the states that were obtained where `mix = 1e-5` was used for the derivation. The left plot in this figure contains the initial state, the harmonic oscillator potential and the reference state $\kappa = 0$ kHz. The right plot contains the desired state together with its double well potential and the corresponding reference state.

Starting the discussion with the initial state one sees that the condensate is represented as a Gaussian located at the origin. Its peak is obviously higher than the peak of the reference Gaussian. As we know, a higher peak means that the width of the Gaussian has to be smaller compared to the reference state due to the conservation of probability. Since this is an ordinary Gaussian distribution the uncertainty in position can be directly related to the packing density. The corresponding uncertainty of the initial state is $\sigma^{\text{initial}}_{\kappa=-2\pi} = 0.159$ μm and it is thus smaller than the uncertainty of the reference state, which is $\sigma^{\text{desired}}_{\kappa=0} = 0.230$ μm. Again, it follows that the packing density is higher for the condensate where attractive interactions are present compared to the non-interacting BEC.

Going on with the desired state one sees that the density function for $\kappa = -2\pi$ kHz has the same shape as the reference state. Because this kind of density function represents the required desired state correctly, it can be used for an optimization calculation.

The difference between these states is that the peaks of the sub-Gaussians of the desired state are again higher than the peaks of the reference state. As we now from the previous section, a greater height corresponds to a smaller width of the sub-Gaussian. It follows that the packing density is then higher for each split part of the BEC than the packing density of the split parts of the reference condensate.

As mentioned in the introduction of this section the extended calculations for this case returned two strategies that modify a BEC in significantly different ways. In both cases the corrected states from figure 5.8 were used as inputs. The same options as for the results of the previous chapters were used for these calculations. The results are presented in figure 5.9. Each subfigure consists of one plot that contains the evolution of the density function and a plot that shows the development of the uncertainty in position. Again, we have added the uncertainty from the reference of figure 5.2. In the following lines we distinguish between the results by using an index (1) when talking about the results from 5.9(a) and index (2) when concerning the results from 5.9(b).

The first part of this discussion considers result (1). As one can see the condensate is split successfully within 10 ms. After the manipulation is over the density function oscillates within the final potential, which can be clearly seen from the color plot. The development of the uncertainty shows that the condensate oscillates during the whole manipulation. At the beginning of the manipulation $\sigma^{(1)}_{\kappa=-2\pi}$ increases almost in the same way as the reference uncertainty. At around $t \approx 5$ ms the uncertainty is drastically increased. One can see that at this point the condensate starts to split into two parts. When the manipulation is over then $\sigma^{(1)}_{\kappa=-2\pi} > \sigma_{\kappa=0}$. The evolution of $\sigma^{(1)}_{\kappa=-2\pi}$ in the time interval $[10, 20]$ ms clearly reflects the oscillations that are visible in the color plot. The oscillations look kind of arbitrary and no clear trend can be seen.

Result (2) shows that this strategy also splits the condensate successfully. During the manipulation the density function starts to spread out around $t = 4$ ms, but then contracts to its initial form. After this, the actual split of the BEC takes place where strong oscillations can be observed. When the manipulation is over the density function does not remain constant. At the beginning of the manipulation the uncertainty in position increases with oscillations. When the density function starts to spread out $\sigma^{(2)}_{\kappa=-2\pi}$ increases, but it is then drastically reduced when the BEC is contracted again. When the actual split occurs the uncertainty drastically increases. The strong oscillations during the actual split are clearly reflected by the evolution of the uncertainty. The evolution of $\sigma^{(2)}_{\kappa=-2\pi}$ in the time interval $[10, 20]$ ms shows a trend. The uncertainty oscillates with a small amplitude when the manipulation is over. But the amplitude of this oscillation increases with time t. A more detailed analysis would be required to tell more about this oscillation, but this goes beyond the scope of this thesis.

What do these two results have in common and what are the differences between them? The first thing is that both results show that these strategies split a condensate successfully. Both uncertainties show that the BECs oscillate when the manipulation is stopped. One difference is that $\sigma^{(1)}_{\kappa=-2\pi}$ indicates that the condensate oscillates already when the manipulation is over. In contrast, the BEC of result (2) starts out with a small oscillation which is then increased. Another difference can be seen from the way

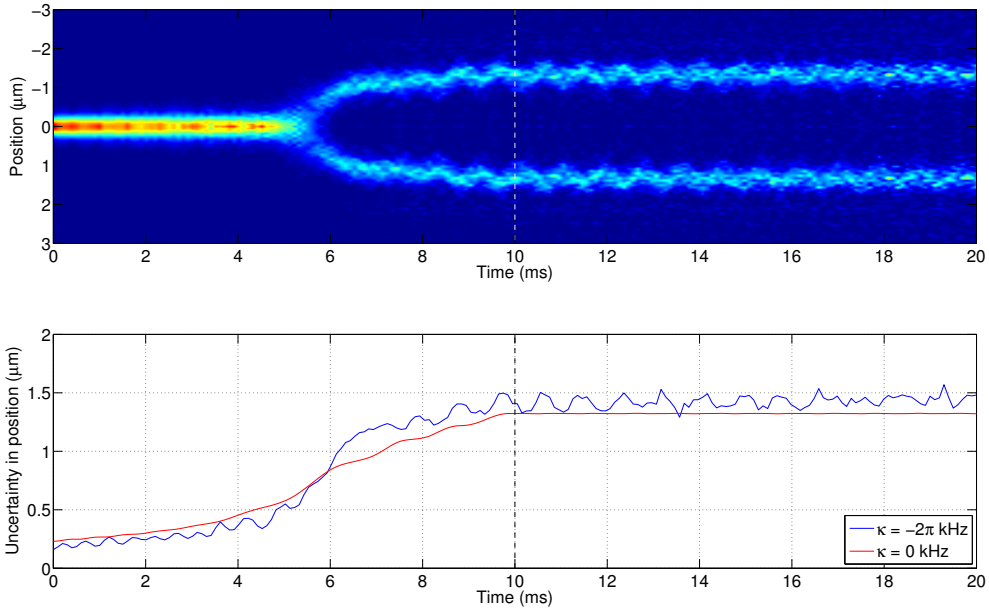

(a) Result (1) of the extended optimization calculation with the corrected inputs.

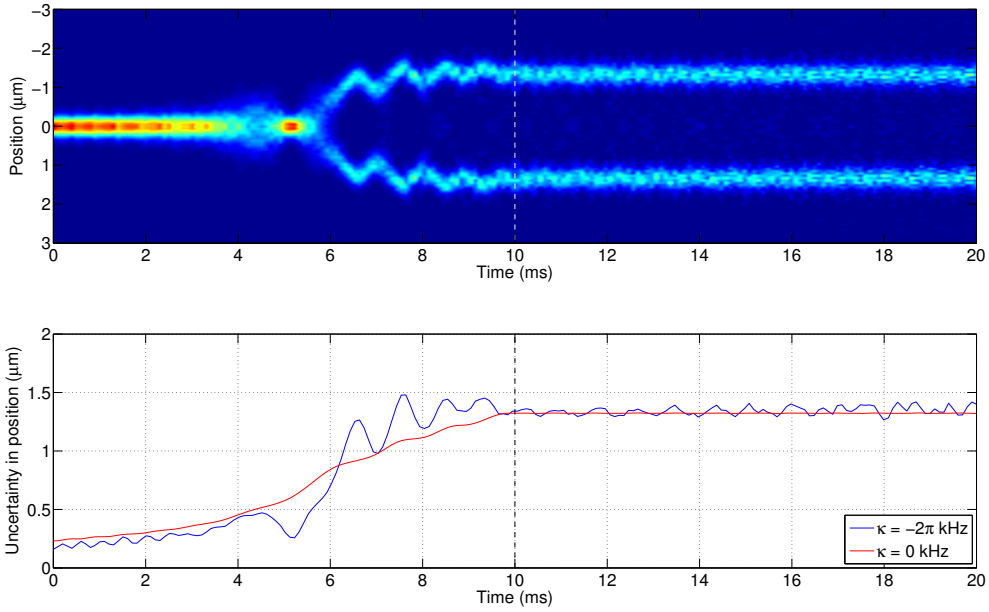

(b) Result (2) of the extended optimization calculation with the corrected inputs.

Figure 5.9: Two different results that were obtained with the same inputs for the optimization routine. The obtained control strategies modify the BEC in contrary ways. Each figure contains the evolution of the density function as well as the development of the uncertainty of position. The solid blue lines are the uncertainties of the modified BEC and the solid red lines are the uncertainty of the reference of figure 5.2.

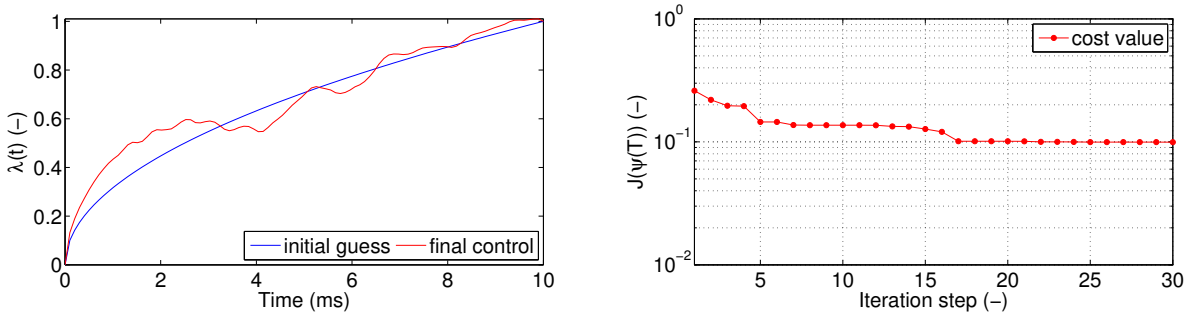

(a) Parameters of result (1).

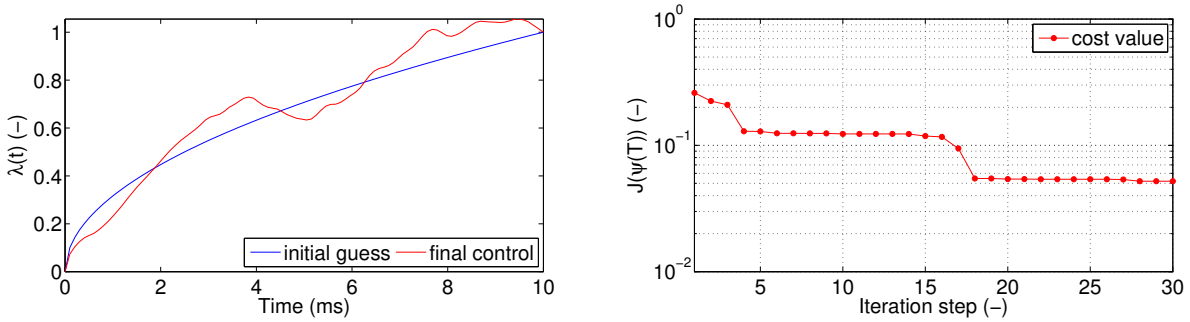

(b) Parameters of result (2).

Figure 5.10: Presentation of the parameters for the two different results (1) and (2). Each subfigure contains the final control strategy as well as the initially guessed strategy in its left plot. The development of the costs are presented in the right plots of each subfigure.

the condensates are split. In the case of result (1) the density function is spread out almost the same until the actual split occurs. Result (2) shows that density function is spread out and contracted before the split takes place. There is also a difference when the actual split has started until the end of the manipulation. In result (1) no significant oscillations during this process can be seen. In contrast, result (2) shows strong oscillations until the manipulation is stopped. An interesting aspect is that this oscillation is drastically reduced in result (2).

It should be clear that all the previously discussed aspects of the results (1) and (2) are directly linked to the corresponding control strategies. This is because only the strategy is responsible for the evolution of the BEC. The strategies that correspond to these results are presented in figure 5.10. Each subfigure contains the final control strategy and the initial guess in the left plot. The right plots then contain the development of the cost functional $J(\psi(T))$ during the optimization. Again, we distinguish between the strategies by the indices (1) and (2) for the subfigure 5.10(a) and 5.10(b).

The final control strategy (1) looks quite different than the initially guessed one. This strategy does not strictly increases, which means that the potential is also varied in the reverse way. In addition, the strategy also varies quite often, which means that there are

several changes in the slope of the curve. Remember, $J(\psi(T))$ contains an extra term that rates the changes of the slope. Although, this term does not contribute as much as the match between the final and desired states, it adds extra costs. The evolution of the costs tells that the strategy was slightly improved. The final costs are $J(\psi(T)) \approx 10^{-1}$ which means that this strategy is inefficient. It has to be mentioned that the toolbox derived a good improvement, because the costs of the first result from figure 3.3(d) were about 0.2. This improve was still not enough although the initial guess was significantly modified.

The final control strategy (2) also does not have very much in common with the initially guessed strategy. Again, this strategy is not a strictly increasing one. Also some changes in the slope are present that add extra costs to $J(\psi(T))$. The evolution of the costs shows a better improvement of the initial guess compared to the costs of strategy (1). The final cost value after the 30th iteration is $J(\psi(T)) \approx 5 \times 10^{-2}$. But as we know, this costs do not represent an efficient manipulation. In this case the great variation of the initial guess did not lead to an efficient strategy.

In both cases, the initially guessed strategy could not be modified after 30 iterations to obtain an efficient strategy. This suggests that the initial guessed control strategy should be reconsidered if one wants to derive a strategy for a BEC with $\kappa = -2\pi$ kHz.

To end this last analysis we shortly summarize the observed aspects from this section: As in the case of $\kappa = -\pi$ the states had to be recalculated with a modified `mix` option. The corrected states then looked similar to the reference states. This means that this states showed the desired aspects of ground states before and after a split process. An extended calculation with this corrected states led to two different results. Both results clearly showed that the BECs can be split successfully within 10 ms. But the condensate also shows oscillations in both cases after the manipulation is over. The corresponding costs were both on the order of 10^{-2} and greater, which characterizes inefficient strategies.

Chapter 6

Conclusion

The goal of this thesis was to tell if the OCTBEC toolbox is capable to derive efficient control strategies to modify BECs with attractive interactions in a way that they are split from a single cluster into two separated parts. The key to this answer was to perform extended calculations by the toolbox. The analyzation of the results was done by focusing on three aspects: The first point was to check if the initial and desired states represent the starting situation for the manipulation correctly. Without suitable inputs, a derivation of an efficient strategy cannot be expected. The second aspect relied on the uncertainty in position. This quantity gave information about the behavior of a BEC during and after the manipulation was finished. Another aspect that helped out was the extension of the actual optimization calculation as well as the recording of the cost values. From this data it was possible to tell if there is room left for further improvements on the strategy, or if new approaches should be made to obtain a better control strategy.

All presented results showed that it is possible to derive strategies that split a BEC in the cases of $\kappa = 0, -\pi, -2\pi$ kHz. But if one is searching for an efficient control strategy, investigations of the inputs as well as modifications of toolbox parameters are required. In the case of $\kappa = 0$ kHz the optimization of the default initial guess strategy led to an applicable efficient strategy. The analysis of the states for $\kappa = -\pi$ kHz showed that the initial and desired states, obtained with default settings, cannot be used to determine an efficient strategy. A recalculation of the states with modified settings returned corrected states, which were then used for the derivation of a new strategy. This new control strategy modifies the BEC in a way that the transition between initial and desired state was made efficient. In addition, the oscillations of the BEC after the manipulation is over was drastically reduced by the new strategy compared to the strategy derived with improper states. The case $\kappa = -2\pi$ kHz then showed that a recalculation of the improper states does not automatically lead to a derivation of a new efficient strategy. Although, an improvement of the strategies was observed, the corresponding costs showed that these strategies are still inefficient. The analysis of the cost history showed that the initially guessed strategy is hard to optimize to achieve a good transition between the states. Because this guess could not be improved as desired by an extended optimization, a different guess for the strategy could lead to a better result.

This analysis covered three exemplary calculations. All results present unique ways to modify BECs in a splitting process that takes place within 10 ms. This means that all the discussed aspects of these manipulations do not hold in general, because there may exist strategies that modify BECs in significantly different ways. The results for the case $\kappa = -2\pi$ actually showed two different strategies, which were derived with the same optimization routine and the same inputs. The reason for this ambiguity was not investigated in more detail, because this would have gone beyond the scope of this thesis. The same also applies for modifications of the splitting time or calculations of results with different guesses for the strategies. Further investigations of these parameters would then give even more insight in the actual behavior of the toolbox and its effects on the final control strategies.

Acknowledgement

First, I would like to thank my supervisor Ulrich Hohenester for giving me the opportunity to work on a present and still growing topic of modern physics. I was able to introduce and expand my knowledge, which i gathered in the past three years of studying physics, in this bachelor thesis.

I also have to thank Georg Jäger who supported me with ideas and took his time for discussions and explanations.

Thanks must also go to Thomas and Florian who provided me with feedback from the point of view of a reader that is new to this topic.

Last but not least, I thank my parents Robert and Eva for enabling me the study of physics in Graz.

Bibliography

[1] U. Hohenester, P. K. Rekdal, A. Borzì, J. Schmiedmayer. *Optimal quantum control of Bose-Einstein condensates in magnetic microtraps.* Physical Review A **75** (2007) 023602.

[2] W. Pauli. *The connection between spin and statistics.* Physical Review **58** (1940) 716.

[3] M. Evans. Statistical Physics, Section 5: Bose-Einstein Condensation, 2009. `http://www2.ph.ed.ac.uk/ mevans/sp/sp5.pdf`

[4] F. Dalfovo, S. Giorgini, L. P. Pitaevskii, S. Stringari. *Theory of Bose-Einstein condensation in trapped gases.* Reviews of Modern Physics **71** (1999) 463.

[5] C. Pethick, H. Smith. *Bose-Einstein Condensation in Dilute Gases.* Cambridge University Press, 2008.

[6] M. H. Anderson, J. R. Ensher, M. R. Matthews, C. E. Wieman, E. A. Cornell. *Observation of Bose-Einstein condensation in a dilute atomic vapor.* science **269** (1995) 198.

[7] M. Trinker, S. Groth, S. Haslinger, S. Manz, T. Betz, S. Schneider, I. Bar-Joseph, T. Schumm, J. Schmiedmayer. *Multilayer atom chips for versatile atom micromanipulation.* Applied Physics Letters **92** (2008) 254102.

[8] J. Fortágh, C. Zimmermann. *Magnetic microtraps for ultracold atoms.* Reviews of Modern Physics **79** (2007) 235.

[9] Q. Effekte. *Materiewellen auf dem Chip.* Physik Journal **8** (2009) 23.

[10] C. Chin, R. Grimm, P. Julienne, E. Tiesinga. *Feshbach resonances in ultracold gases.* Reviews of Modern Physics **82** (2010) 1225.

[11] C. Bradley, C. Sackett, R. Hulet. *Bose-Einstein condensation of lithium: Observation of limited condensate number.* Physical Review Letters **78** (1997) 985.

[12] S. Inouye, M. Andrews, J. Stenger, H.-J. Miesner, D. Stamper-Kurn, W. Ketterle. *Observation of Feshbach resonances in a Bose–Einstein condensate.* Nature **392** (1998) 151.

[13] K. Strecker, G. Partridge, A. Truscott, R. G. Hulet. *Tunable interactions in ultracold Bose gases.* Advances in Space Research **35** (2005) 78.

[14] J. Grond. Optimal quantum control of trapped Bose-Einstein condensates. Graz, Univ., Diss., 2010.

[15] G. Jäger. Optimal Quantum Control of Bose-Einstein Condensates. Graz, Univ., Diss., 2015.

[16] U. Hohenester. *OCTBEC—A Matlab toolbox for optimal quantum control of Bose–Einstein condensates.* Computer Physics Communications **185** (2014) 194.

[17] C. M. Dion, E. Cancès. *Ground state of the time-independent Gross–Pitaevskii equation.* Computer physics communications **177** (2007) 787.